4.2.2 Simulations Results

All simulations, including the proposed and original active inductor, were carried out using Agilent-ADS simulator with TSMC 0.25um 1P5M CMOS model biased at 2.5 V. In Fig. 4.18, the curve of the proposed active inductor is shifted outer and toward right comparing with that of the original active inductor. Fig. 4.18 indicates the performances of the proposed active inductor outperform the original active inductor. The inductance, the Q value, the equivalent loss, and the layout are shown in Figs. 4.19, 4.20, and 4.21, respectively.
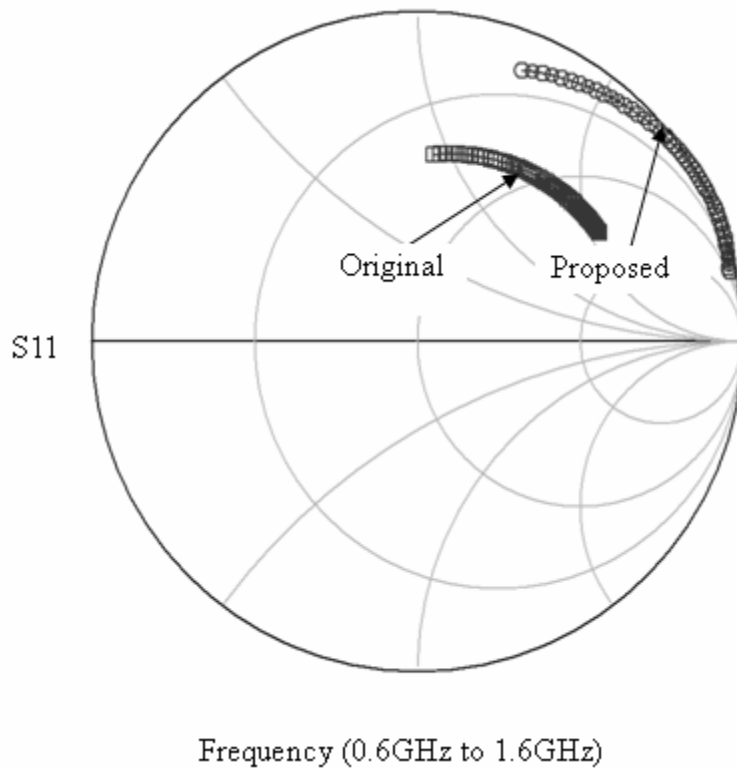

Fig. 4.18 Microwave performance of active inductor (S11)

From the simulation results, we can summarize that the equivalent input loss resistance is reduced in the proposed active inductor. The Q value, the inductance, and the operating frequency are also increased and both the circuit complexity and power consumption are also improved. The results of this active inductor have 1mΩ of minimum total equivalent loss, 3E5 maximum Q-value, and inductance value from 20nH to 45nH in the RF range from 0.6GHz to 1.6GHz. Power consumption is only about 1.76mW under 2.5V supply voltage, which is smaller than that of the original active inductor using negative impedance converter (~3.76mW). Therefore this proposed active inductor circuit only uses three components, simpler than the original active one applying the negative impedance converter circuit to improving the performances of active inductor. Consequently, both circuit complexity and power dissipation of the proposed circuit are improved significantly.
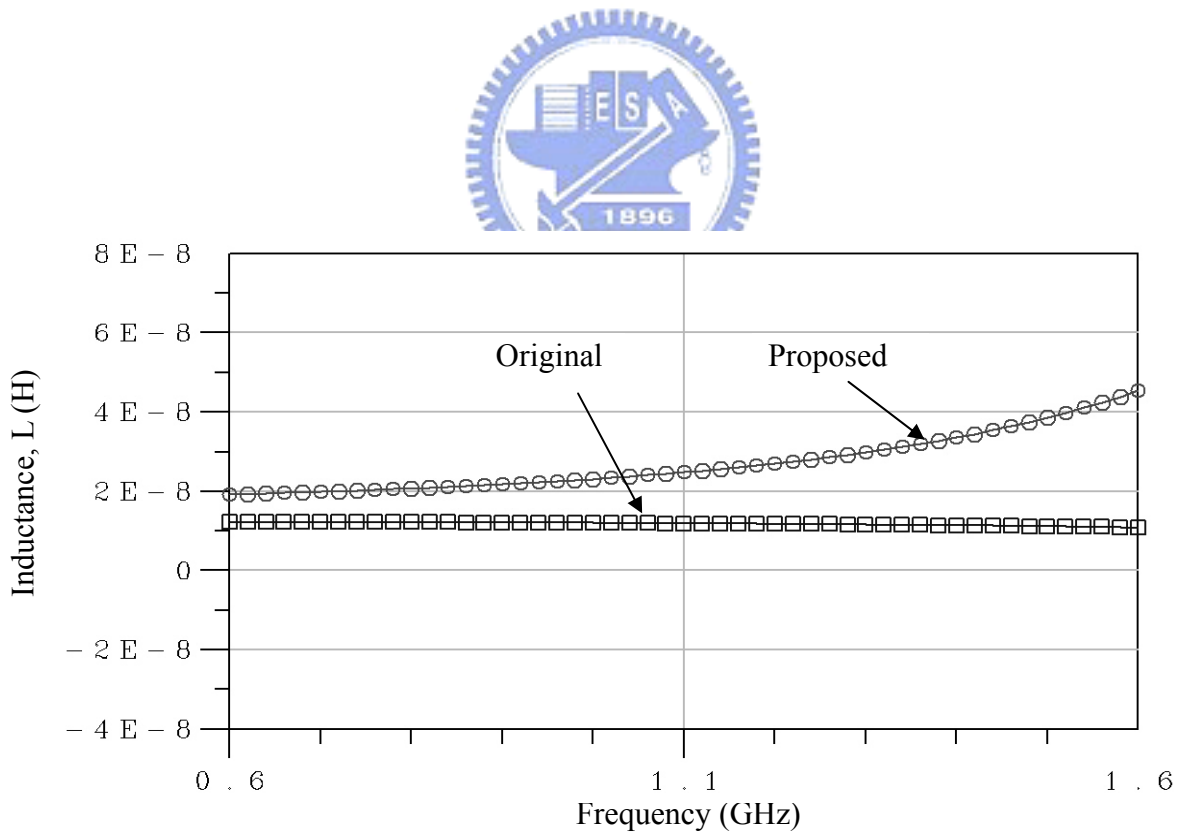

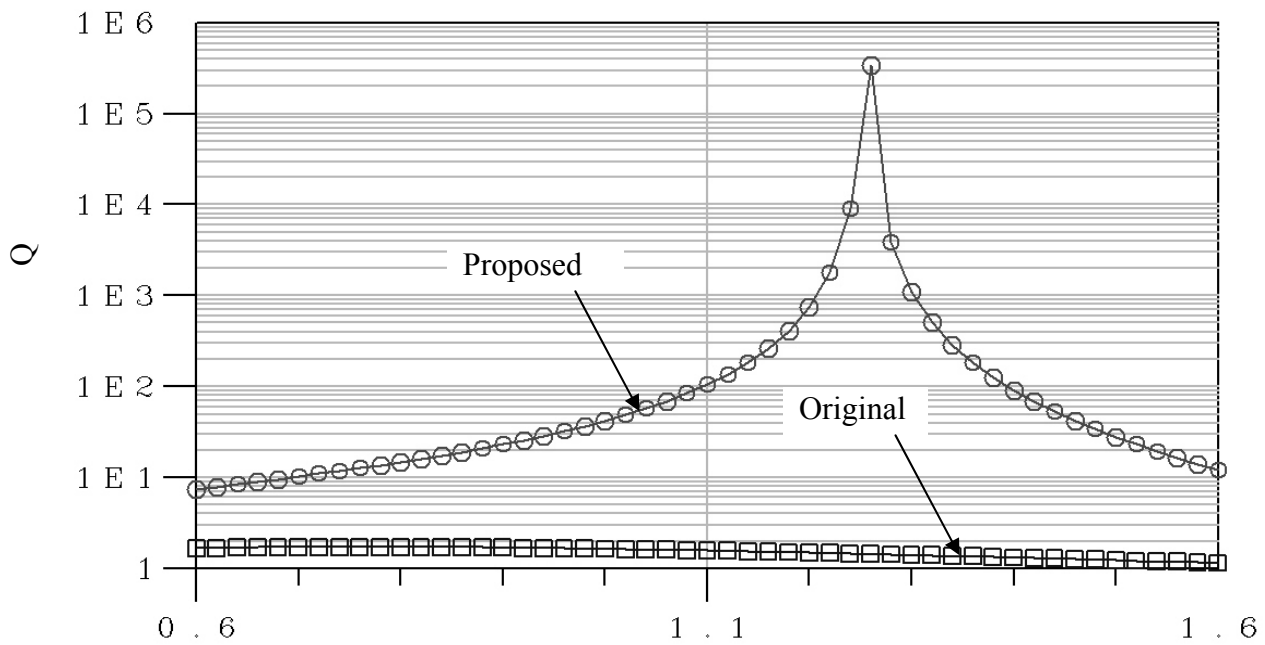Fig. 4.19 Inductance L of active inductor
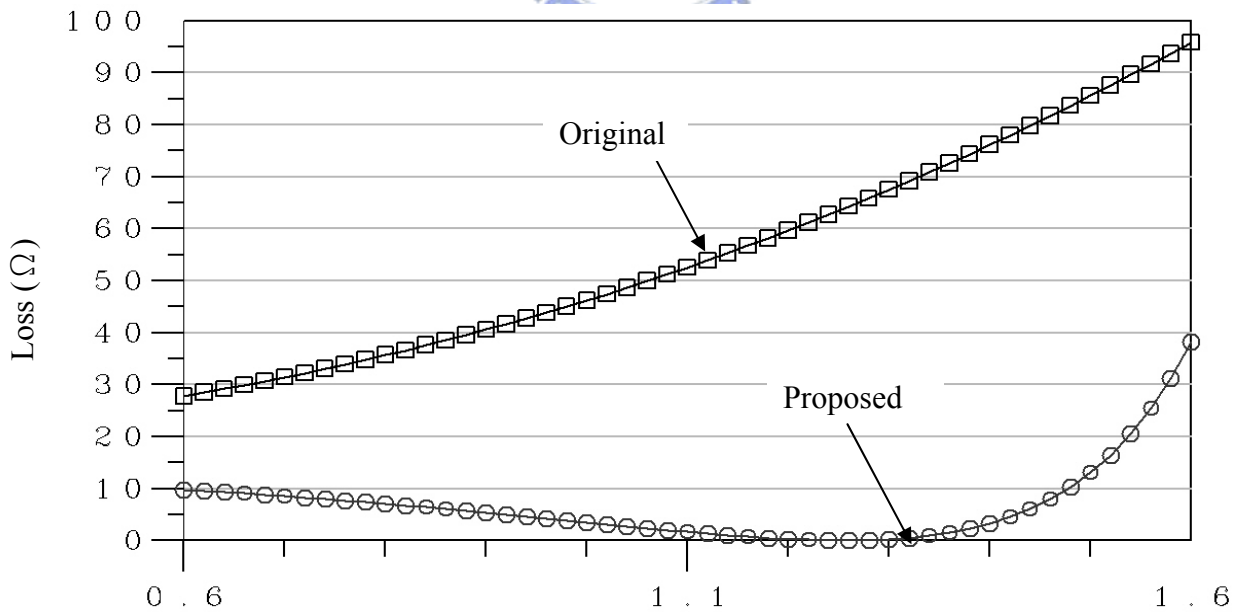
Fig. 4.20 Q value of active inductor

Fig. 4.21 Equivalent loss of active inductor

TABLE 4.3 COMPARISONS BETWEEN IMPROVED AND ORIGINAL @1.25GHZ

	Improved	Original
Q	3E5	1.2
Loss (Ohm)	1E-3	6.5
Inductance (H)	30n	10n
Power Consumption (mW)	3.76	4

4.2.3 Discussion

A novel RF CMOS high Q active inductor for RF applications with simple loss compensation technique has been proposed. According to simulation results, a simple and effective active inductor circuit can be easily obtained. This active inductor circuit can eventually perform high Q value, large inductance, higher operating frequency, simple circuit, and low power consumption. This loss compensation technique is highly desirable and applicable in RF amplifiers, active resonators, and active filters, etc. The comparisons between improved and original at 1.25GHz is shown in TABLE 4.3.

4.3 Loss Compensation in RF CMOS Active Inductor Using a Capacitor

In RF CMOS active inductor applications, Q-value, inductance (L), and operating frequency is limited by the loss. To solve these problems, many Q-enhancement active inductor circuits have been proposed [36-39]. Although these Q-enhancement designs improved the performance of the active inductor, the complexity and the power consumption are greatly increased. In addition, an active inductor based on CMOS generalized impedance converter (GIC) and applied a simple loss compensation circuit to simultaneously reduce

series/parallel and parasitic capacitance loss has been also proposed [42]. Though the Q-value, the inductance, the operating frequency, the complexity, and the power consumption of this active inductor are greatly improved, the characteristics of the active inductor became seriously degraded when MOSFET active devices replaces the ideal current sources of the active inductor. This circuit is shown in Fig. 4.21(a).

In this work, a simple technique is proposed. We use only a capacitor to overcome the decaying characteristics caused by the active devices instated of using ideal current sources. Theoretical analysis and simulation results show that the performances of this active inductor are significantly improved and are better than those of previous literatures. The improved circuit design of the active inductor is described in section 4.3.1. The simulation results of the proposed active inductor are expressed in section 4.3.2. Finally, the discussion is given in section 4.3.3.

4.3.1 Circuit Design

Figure 4.22 (a) and (b) show the active inductor and the small-signal equivalent circuit respectively. Based on the literature [42], the ideal current sources of this active inductor circuit are replaced by MOSFET active devices (M_3 and M_4). Although the performances are significantly improved by using loss compensated techniques in the literature [42], the performance collapsed when the ideal current sources are substituted for the practical MOSFET active devices (M_3 and M_4) for integrated circuit (IC) fabrication.
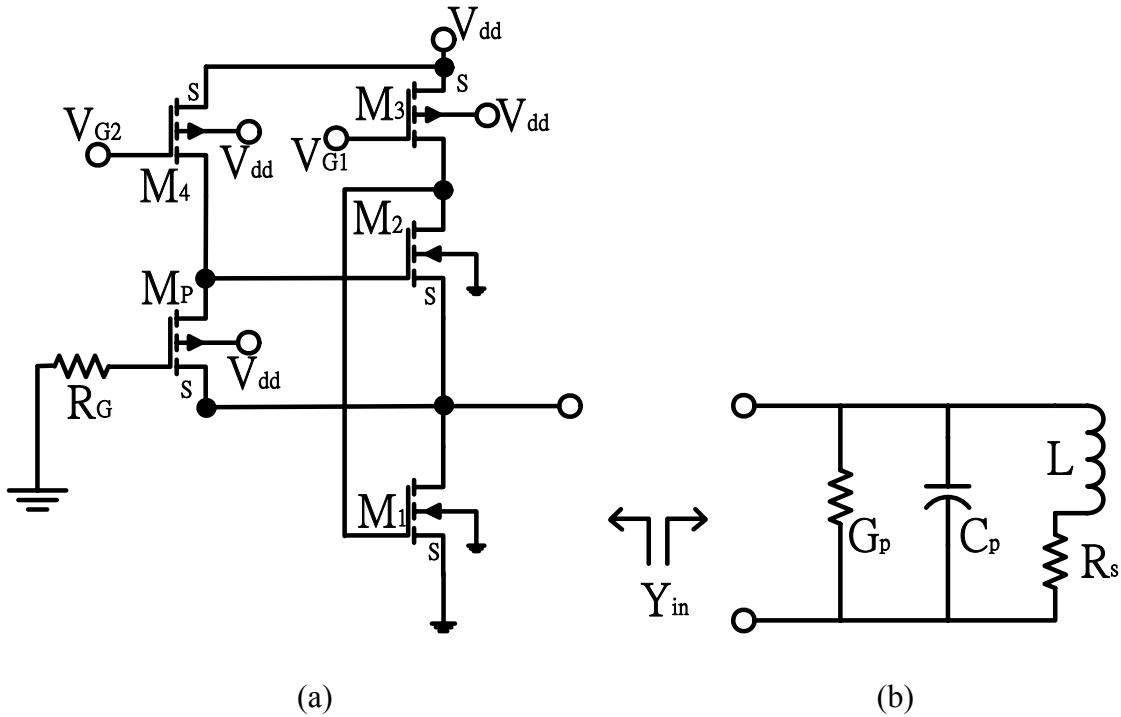
(a)   (b)

Fig. 4.22 The original active inductor circuit and small signal equivalent circuit

In Fig. 4.22 (a), the non-ideal characteristics of the transistors M_3 and M_4, such as the g_{ds} (the conductance of drain to source of the transistor) and the capacitance C_{gs} (between the gate and the source of the transistor) increase the parallel loss (G_P) and the series losses (R_S) of the active inductor shown in Fig. 4.22(b). For a small signal, the finite conductance (g_{ds}) and the capacitance (C_{gs}) of the transistors (M_3 and M_4) cause the loss paths from the drain of M_P and M_2 to the ground, the signal of generating the inductance characteristic of the active inductance will lost through the loss paths. Therefore, the loss paths arise in the increase of the parallel loss and the series loss. Consequently, the performances of the active inductor mentioned in literature [42] would cause seriously decay when the ideal current sources are replaced by the practical MOSFETs current sources.

Theoretically, we can neglect the gate-drain capacitance (C_{gdi}) and all identical MOSFETs dimensions. When we assume $\omega R_g C_{gsMp} << 1$, $g_{mi} >> g_{dsi}$ and $C_{gsM_1} = C_{gsM_2} = C_{gsM_3} = C_{gsM_4} = C_{gsM_P} = C_{gs}$, we can then derive the equivalent input

conductance (Y_{in}) of the active inductor. This design is shown in Fig. 4.22 (a), and the equation Y_{in} can be expressed as Eq. (4.10).

$$Y_{in} \approx G_P + sC_P + \frac{1}{sL+R_S} \approx (g_{dsM_1} + g_{dsM_2} + g_{dsM_4} + g_{mM_4}) + s(\frac{3C_{gs}}{2})$$

(4.10)

$$+ \frac{g_{mM_1}g_{mM_2}g_{mM_3}g_{mM_4}g_{mM_P}(g_{mM_1}g_{mM_2} + g_{dsM_2}g_{mM_P})}{s[C_{gs}(g_{mM_1}g_{mM_2}g_{mM_4} + g_{mM_2}g_{mM_3}g_{mM_P})(g_{mM_1}g_{mM_2} + g_{dsM_2}g_{mM_P})] + [(g_{dsM_2} + g_{dsM_3} + g_{mM_3})g_{mM_1}g_{mM_2}g_{mM_3}g_{mM_4}g_{mM_P}]}$$

The g_{dsMi} and g_{mMi} are the output conductance and transconductance of the corresponding transistors, and C_{gs} is the gate source capacitance. According to Eq. (4.10), the equivalent input conductance is shown in Fig. 4.22 (b), where the corresponding component values can be expressed as below:

$$G_p \approx g_{dsM_1} + g_{dsM_2} + g_{dsM_4} + g_{mM_4} \approx g_{mM_4}$$

(4.11)

$$R_S \approx \frac{g_{dsM_2} + g_{dsM_3} + g_{mM_3}}{g_{mM_1}g_{mM_2} + g_{dsM_2}g_{mM_P}} \approx \frac{g_{dsM_2} + g_{dsM_3} + g_{mM_3}}{g_{mM_1}g_{mM_2}}, \; (if \; g_{dsM_2}g_{mM_P} << g_{mM_1}g_{mM_2})$$

(4.12)

$$C_p \approx \frac{3C_{gs}}{2}$$

(4.13)

$$L \approx \frac{C_{gs}(g_{mM_1}g_{mM_4} + g_{mM_3}g_{mM_P})}{g_{mM_1}g_{mM_3}g_{mM_4}g_{mM_P}}$$

(4.14)

From Eq. (4.11) and Eq. (4.12), the parallel loss (G_P) of g_{mM_4} and the series loss (R_S)

of $\dfrac{g_{dsM_2} + g_{dsM_3} + g_{mM_3}}{g_{mM_1}g_{mM_2}}$ are significantly increased when comparing with literature [53] and

the Q-value of the active inductor is greatly reduced. From Eq. (4.13) and Eq. (4.14), the capacitance C_P is raised, and the inductance L is greatly decayed as well.

In order to improve the performance, a schematic diagram of our proposed active inductor circuit is shown in Figure 4.23. Except for adding capacitor C_N, the active inductor is similar to previous active inductor, given in Fig. 4.22.
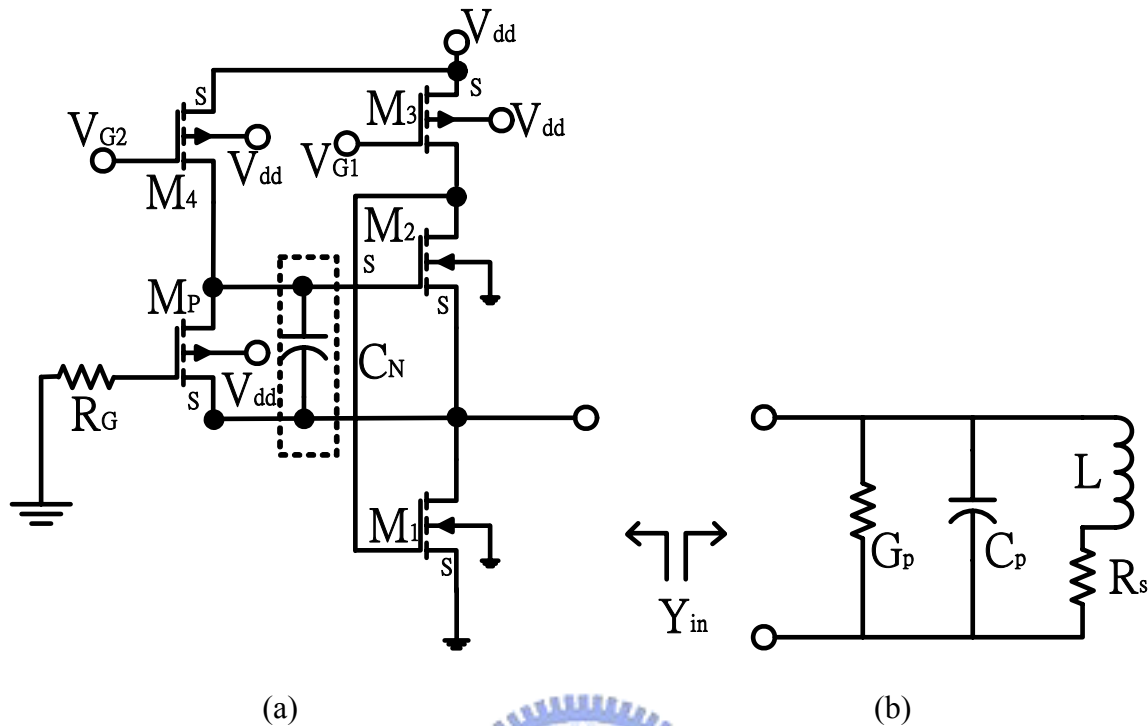
(a)   (b)

Fig. 4.23 The proposed active inductor circuit and small signal equivalent circuit

In Fig. 4.23 (a), the design only uses a feedback capacitor (C_N) for compensating the loss, which is caused by MOSFET current source (M_3 and M_4). Transistors M_1, M_2, capacitor C_N, resistor R_G, and transistor M_P are the components of the proposed active inductor circuit. Transistors M_3 and M_4 are the current source of the inductor. The circuit operation of the inductor includes negative feedback, positive feedback, and current pumping to obtain inductivity impedance and to reduce the loss of the active inductor. M_1 and M_2 are the components of the negative feedback operation path for converting the input voltage back to the input current. This mechanism realizes input inductivity impedance of the active inductor. The positive feedback and current pumping path pass through C_N and M_P and this positive feedback creates negative conductance and raises the current for compensating the loss of the active inductor. Therefore, the Q-enhancement obtained in the active inductor is accomplished by adding an equivalent negative conductance into the input terminal. This

-73-

negative conductance is generated by the interaction between C_N and the current pumping circuit comprising M_P and R_G. Consequently, the loss is greatly reduced, and the Q value is enormously improved. When considering parameters C_{gs}, g_{ds}, g_m, and C_N for analyzing the proposed circuit and assuming all identical MOSFETs dimensions, $\omega R_G C_{gs} << 1$, $g_{mi} >> g_{dsi}$, $\omega << g_{mP}/(C_{gs}+C_N)$, and $C_{gsM_1} = C_{gsM_2} = C_{gsM_3} = C_{gsM_4} = C_{gsM_P} = C_{gs}$, we can express Y_{in} as Eq. (4.15).

$$Y_{in} \approx G_P + sC_P + \frac{1}{sL + R_S} \approx [(g_{dsM_1} + g_{dsM_2} + g_{dsM_4} + g_{mM_4}) - \frac{\omega^2 C_{gs} C_N}{g_{mM_p}}] + \frac{sC_{gs}}{3}$$
$$+ \frac{g_{mM_1} g_{mM_2} g_{mM_3} g_{mM_4} g_{mM_P}(g_{mM_1} g_{mM_2} + g_{dsM_2} g_{mM_P})}{\lambda} \tag{4.15}$$

$$\lambda = s[(C_{gs} + C_N)(g_{mM_1} g_{mM_2} g_{mM_4} + g_{mM_2} g_{mM_3} g_{mM_P})(g_{mM_1} g_{mM_2} + g_{dsM_2} g_{mM_P})]$$
$$+ [(g_{dsM_2} + g_{dsM_3} + g_{mM_3} - \frac{\omega^2 C_{gs} C_N}{g_{mM_P}})g_{mM_1} g_{mM_2} g_{mM_3} g_{mM_4} g_{mM_P}]$$

In Eq. (4.15), the small signal equivalent circuit model of the proposed active inductor circuit can also be written as Fig. 4.23 (b). The values of each component are expressed below.

$$G_p \approx (g_{dsM_1} + g_{dsM_2} + g_{dsM_4} + g_{mM_4}) - \frac{\omega^2 C_{gs} C_N}{g_{mM_p}}$$
$$\approx g_{mM_4} - \frac{\omega^2 C_{gs} C_N}{g_{mM_p}} \tag{4.16}$$

$$R_S \approx \frac{(g_{dsM_2} + g_{dsM_3} + g_{mM_3}) - \dfrac{\omega^2 C_{gs} C_N}{g_{mM_P}}}{g_{mM_1} g_{mM_2} + g_{dsM2} g_{mM_P}} \approx \frac{(g_{dsM_2} + g_{dsM_3} + g_{mM_3}) - \dfrac{\omega^2 C_{gs} C_N}{g_{mM_P}}}{g_{mM_1} g_{mM_2}} \tag{4.17}$$

$$C_P \approx \frac{C_{gs}}{3} \tag{4.18}$$

$$L \approx \frac{(C_{gs} + C_N)(g_{mM_1} g_{mM_4} + g_{mM_3} g_{mM_P})}{g_{mM_1} g_{mM_3} g_{mM_4} g_{mM_P}} \tag{4.19}$$

In Eq. (4.16) and Eq. (4.17), the parallel conductance loss (G_P) and series resistance loss (R_S) are changed from g_{mM_4} to $g_{mM_4} - \dfrac{\omega^2 C_{gs} C_N}{g_{mM_P}}$ and from $\dfrac{g_{dsM_2} + g_{dsM_3} + g_{mM_3}}{g_{mM_1} g_{mM_2}}$

to $\dfrac{(g_{dsM_2} + g_{dsM_3} + g_{mM_3}) - \dfrac{\omega^2 C_{gs} C_N}{g_{mM_P}}}{g_{mM_1} g_{mM_2}}$ respectively and the negative term in the equation

reduces the parallel loss and the series loss. In Eq. (4.18), the reduced capacitance is $\dfrac{C_{gs}}{3}$,

and it increases the operating frequency. In Eq. (4.19), the equivalent inductance will be also

increased from $\dfrac{C_{gs}(g_{mM_1} g_{mM_4} + g_{mM_3} g_{mM_P})}{g_{mM_1} g_{mM_3} g_{mM_4} g_{mM_P}}$ to $\dfrac{(C_{gs} + C_N)(g_{mM_1} g_{mM_4} + g_{mM_3} g_{mM_P})}{g_{mM_1} g_{mM_3} g_{mM_4} g_{mM_P}}$ by a factor

of $\dfrac{C_N(g_{mM_1} g_{mM_4} + g_{mM_3} g_{mM_P})}{g_{mM_1} g_{mM_3} g_{mM_4} g_{mM_P}}$. In consequence, the performances of the active inductor are

improved by using a capacitor (C_N). If the circuit components are properly chosen, a higher

Q-value, higher inductance, and higher operating frequency can be realized.

4.3.2 Simulation Results

All simulations are implemented via an Aligent-ADS simulator. The active devices are

modeled by TSMC 0.25um CMOS process at 2.5V. All transistors have the same dimensions,

where the length and width of each MOSFET are 0.24 um and 40 um, respectively. The value

of the components are designed to have R_G=550Ω and C_N=0.73PF. The scattering parameter

S11 performance of the active inductor is shown in Fig. 4.24. It can be seen that the curve of

the proposed active inductor, which is added one capacitor (C_N) for compensating the loss, is

inclined to the outside of circle when the frequency is between 0.6GHz and 1.3GHz. This

result indicates that the loss is decreased, and the Q-value is greatly increased.

The curves of the inductance, the equivalent loss, the Q-value, and the layout are

shown in Figs. 4.25, 4.26, 4.27, and 4.28 respectively. These curves indicate that in the range of 0.6GHz to 1.3GHz, the inductance value varies from 50nH to 450nH, in which it has large enough inductance for RF circuit applications. The minimum equivalent loss is about 1.4E-6Ω, and maximum Q-value is about 1.2E8. Furthermore, Fig. 4.25, Fig. 4.26 and Fig. 4.27 show the comparisons of the inductance (L), the loss, and the Q-value between the proposed active inductor, which is added a capacitor (C_N) and the active inductor in the literature [35], in which the practical current sources replace the ideal current sources and the capacitor (C_N) does not added in the circuit. The results shown in Fig. 4.25, Fig. 4.26 and Fig. 4.27 are because the non-ideal factors of the MOSFETs (M_3 and M_4) generate the loss paths. Consequently, the performance of the proposed active inductor is much better than that of active inductor, in which the practical current sources replace the ideal current sources and without using the capacitor (C_N) to compensate the loss of the active inductor circuit.
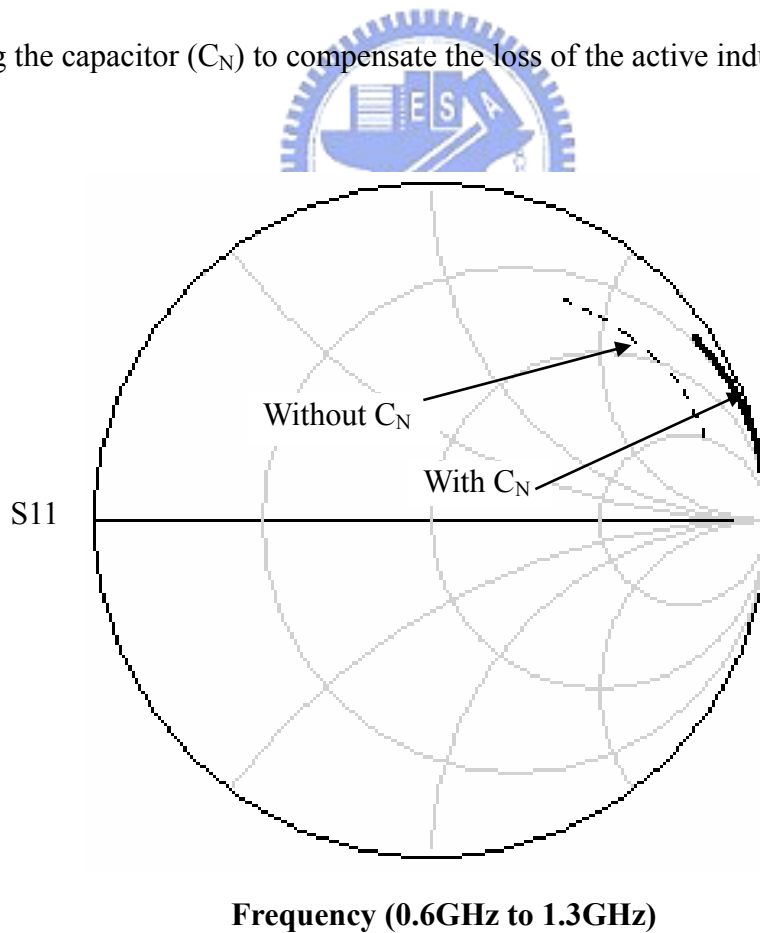

Frequency (0.6GHz to 1.3GHz)

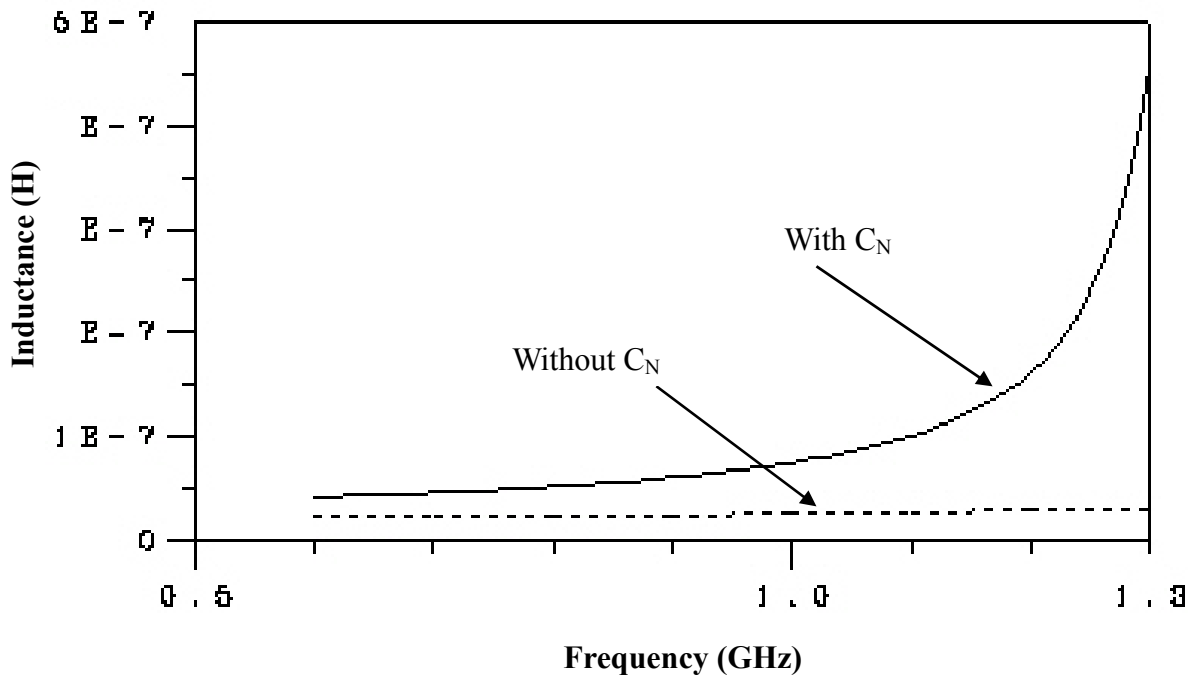Fig. 4.24 S11 of the proposed active inductor circuit

Fig. 4.25 Inductance of the proposed active inductor circuit

The active inductor shows a significant improvement. The power consumption is only about 1.9mW under 2.5 V supply voltage, which has less power consumption in this active inductor. Furthermore, in this active inductor, the external bias voltages are used to tune the characteristics of the active inductor due to the variation in the circuit implementation. Therefore, the performance demand can be satisfied and is independent of the process variation. The layout of the proposed active inductor is shown in Fig. 4.28. From the Fig. 4.28, the size of the proposed active inductor, which includes the IO pads, is about 1126 um × 605 um.
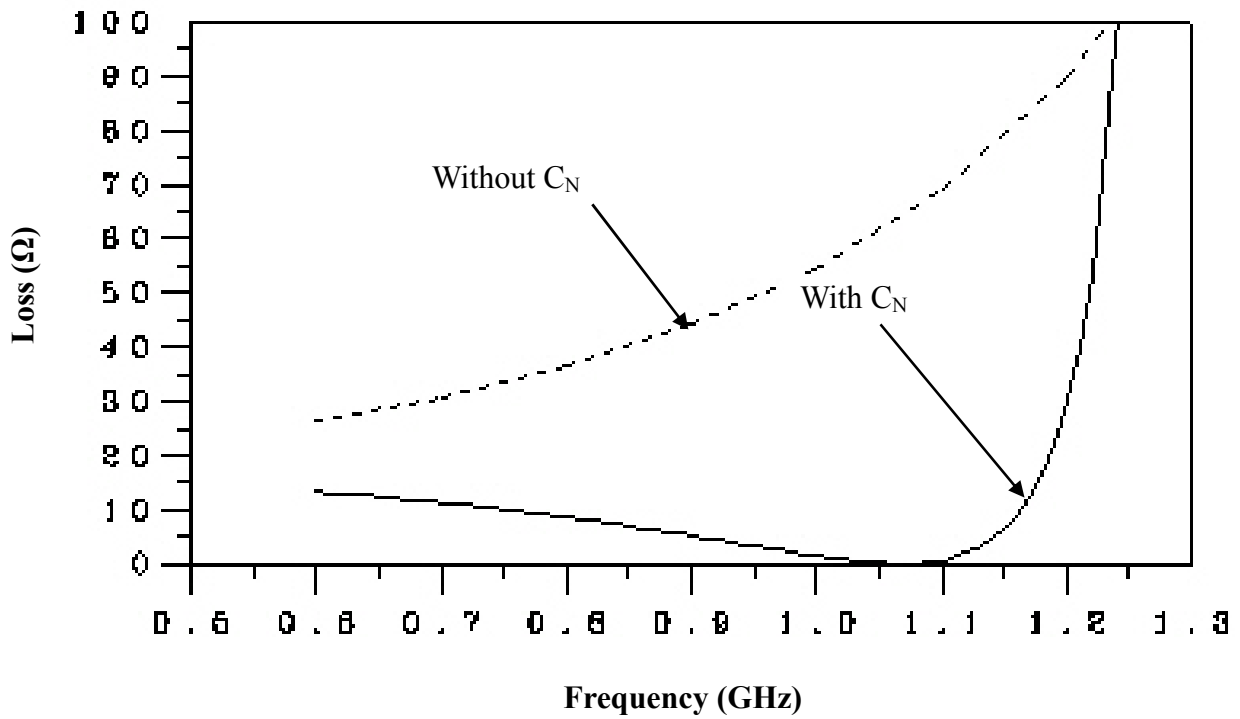
Fig. 4.26 Equivalent loss of the proposed active inductor circuit
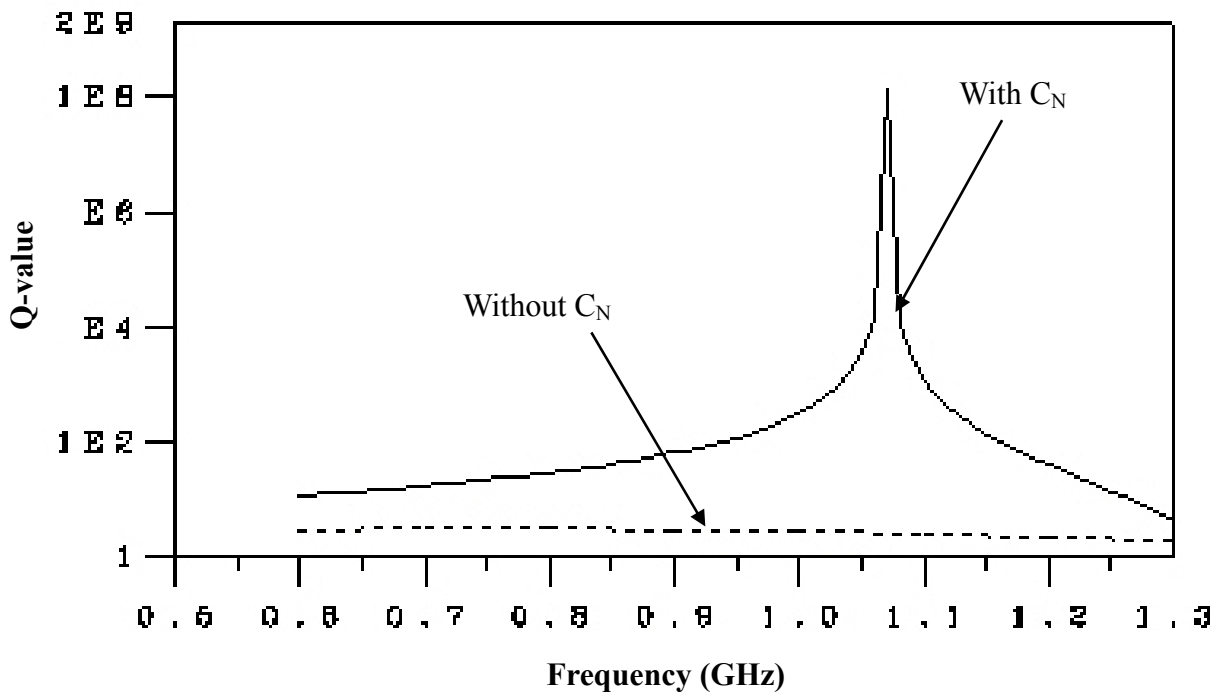
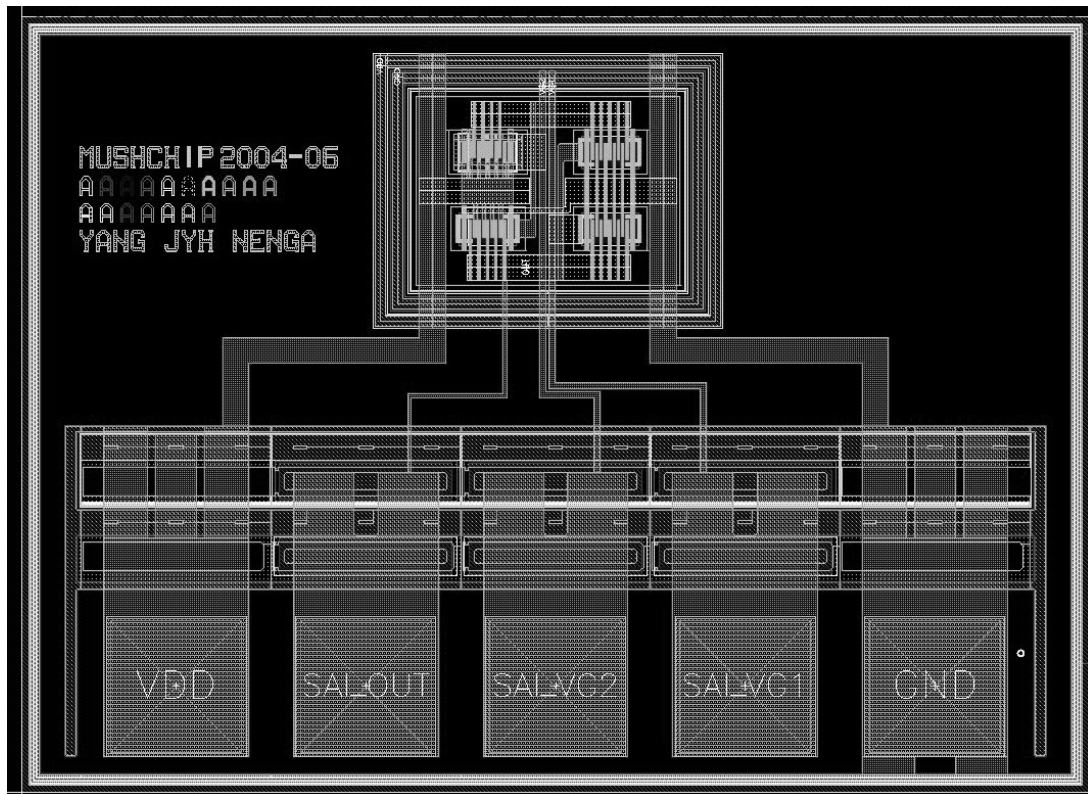

Fig. 4.27 Q-value of the proposed active inductor circuit

Fig. 4.28 Layout of the proposed active inductor circuit

TABLE 4.4 COMPARISON BETWEEN IMPROVED AND ORIGINAL @1.05GHZ

	Improved	Original
Q	1.2E8	1.5
Loss (Ohm)	1.4E-6	80
Inductance (H)	75n	25
Power Consumption (mW)	1.9	2.2

4.3.3 Discussion

A CMOS high Q-value RF active inductor using a simple feedback loss compensation circuit is proposed. We use one capacitor in the feedback loop to compensate the loss of CMOS active devices and use external bias voltage to compensate the variation in IC fabrication. As a result, a higher Q-value, inductance value, and reasonable power consumption under 2.5V supplies voltage are achieved between the 0.6GHz to 1.3GHz

frequency. Simulation results show that our proposal achieves better performance indices compared to those having the same active inductor structure published earlier. The comparisons between improved and original at 1.05GHz is shown in TABLE 4.4.

4.4 An Improving Active Inductor Using a Resistor

In RF CMOS active inductor circuits, Q-value and inductance (L) are limited by the loss. To solve these problems, a cascode technique has been used to improve the Q-value [34, 41]. Although, this Q-enhancement design improved the performance of the active inductor, the introduction of the additional high frequency poles and zeros into signal path can lead the circuit to instability [34]. In additional, the negative resistance in active inductor design to compensate the internal loss of the active inductor has also been proposed [38, 39]. Though, the Q-value was greatly improved, this negative resistance method requires an additional circuit and it causes an increase in power consumption. However, a high-Q active inductor using a simple loss compensation technique can solve the above problems.

In this work, an improved high-Q active inductor by adding one resistor in the feedback path is proposed. In this active inductor circuit, the resistor interacts with transistors for generating a gain factor. The gain factor will reduce the internal loss of the active inductor and increase the inductance of the active inductor. As a result, the performance of the active inductor can be significantly improved. Furthermore, the power consumption is reduced and the circuit complexity is simplified when comparing with the previously mentioned results. The improved circuit design of the active inductor is described in section 4.4.1. The simulation results of the proposed active inductor are expressed in section 4.4.2. Finally, the discussion is given in section 4.4.3.

4.4.1 Circuit Design

The simplest active inductor and the small-signal equivalent circuit based on a gyrator topology are shown in Fig. 4.29(a) [33]. This circuit can only produce a very small Q value (about $2 \sim 3$), which is still too low for practical applications. At high frequency, the circuit is equivalent to a lossy resonator as shown in Fig. 4.29(b). Based on the assumption of $C_{gsi} >> C_{gdi}$, the equivalent input conductance (Y_{in}) can be expressed as Eq. (4.20).

$$Y_{in} \approx (g_{ds2} + g_{m1}) + sC_{gs1} + \frac{g_{m1}g_{m2}}{sC_{gs2} + g_{ds1}} \tag{4.20}$$

From Eq. (4.20), the component values of the lossy resonator as shown in Fig. 4.29(b) are described as below.
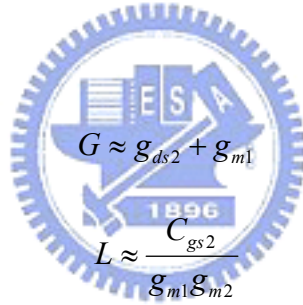
$$G \approx g_{ds2} + g_{m1} \tag{4.21}$$

$$L \approx \frac{C_{gs2}}{g_{m1}g_{m2}} \tag{4.22}$$

$$R_s \approx \frac{g_{ds1}}{g_{m1}g_{m2}} \tag{4.23}$$

$$C \approx C_{gs1} \tag{4.24}$$

where g_{mi}, g_{dsi}, and C_{gsi} are the transconductance, output conductance, and gate-source capacitance of correspondence MOSFET transistors, respectively. In Eq. (4.21), the increasing parallel conductance loss of G will reduce the Q-value of the active inductor. Therefore, in order to improve the Q-value and the inductance (L), an improved high-Q active inductor with a feedback resistor is proposed for reducing the parallel conductance loss of G.
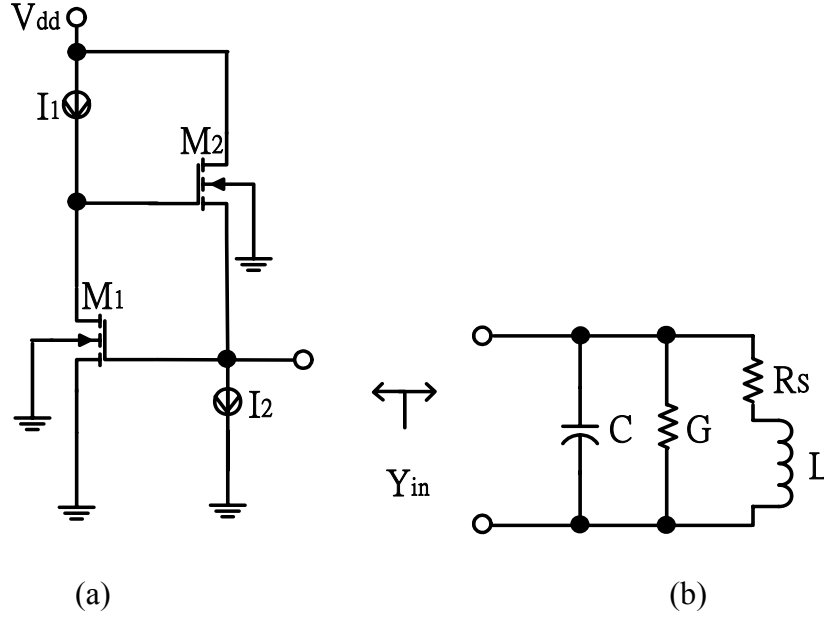
Fig. 4.29 Original active inductor circuit and small signal equivalent circuit

The improved high-Q active inductor circuit is illustrated in Fig. 4.30. This circuit is composed of common source transistor M_1, common drain transistor M_2, feedback resistor R_f, and two biasing current sources I_1 and I_2. Feedback resistor R_f and transistor M_1 construct a gain network. This network produces a gain factor to reduce the parallel loss conductance (G) Furthermore, the internal loss of the inductor will be decreased and then the Q value can be increased. In additional, the inductance (L) is also increased because of the feedback resistor R_f generating a gain factor. At high frequency, this circuit is equivalent to a lossy resonator as well, which is shown in Fig. 4.29 (b). When considering parameters C_{gs}, g_{ds}, g_m, and R_f for analyzing the proposed circuit and assuming all identical MOSFETs dimensions, $C_{gsi} >> C_{gdi}$, $g_{mi} >> g_{dsi}$, and $\omega C_{gs2} >> g_{ds1}$, we can express Y_{in} as Eq. (4.25).

$$Y_{in} \approx (g_{ds2} + \frac{g_{m1}}{1 + g_{ds1}R_f}) + sC_{gs1} + \frac{g_{m1}g_{m2}}{sC_{gs2}(1 + g_{ds1}R_f) + g_{ds1}} \qquad (4.25)$$
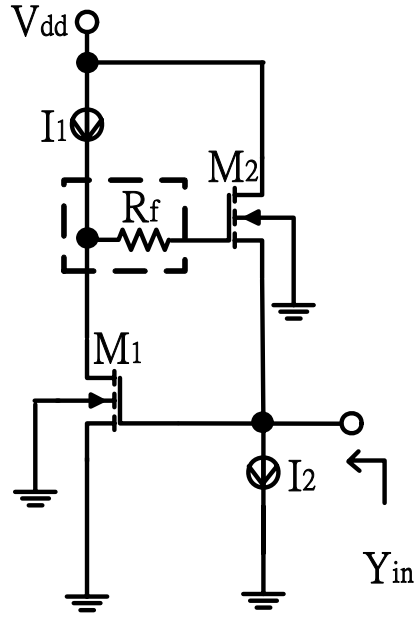
Fig. 4.30 Proposed active inductor with loss compensation

In Eq. (4.25), the small signal equivalent circuit model of the proposed active inductor circuit can also be modeled as Fig. 4.29(b). The values of each component are expressed below.

$$G \approx g_{ds2} + \frac{g_{m1}}{1 + g_{ds1}R_f} \tag{4.26}$$

$$L \approx \frac{C_{gs2}(1 + g_{ds1}R_f)}{g_{m1}g_{m2}} \tag{4.27}$$

$$R_s \approx \frac{g_{ds1}}{g_{m1}g_{m2}} \tag{4.28}$$

$$C \approx C_{gs1} \tag{4.29}$$

In Eq. (4.26), the effect of the factor, $(1 + g_{ds1}R_f)$, is designed to be a value greater than unity. The equivalent parallel conductance loss (G) changes from $g_{ds2} + g_{m1}$ to $g_{ds2} + \dfrac{g_{m1}}{1 + g_{ds1}R_f}$ and the loss is minimized by a $(1 + g_{ds1}R_f)$ factor. In the Eq.

(4.27), the equivalent inductance changes from $\dfrac{C_{gs2}}{g_{m1}g_{m2}}$ to $\dfrac{C_{gs2}(1+g_{ds1}R_f)}{g_{m1}g_{m2}}$, and the inductance are also increased by a $(1+ g_{ds1}R_f)$ factor. Therefore, the Q-value and the inductance (L) of the inductor are greatly increased. As a result, the performance of the inductor can be significantly improved by using a simple loss compensation of a feedback resistor (R_f). Furthermore, the circuit design of the active inductor is simpler than others published earlier. If the circuit components are properly chosen, a higher Q-value and a higher inductance value can be realized.
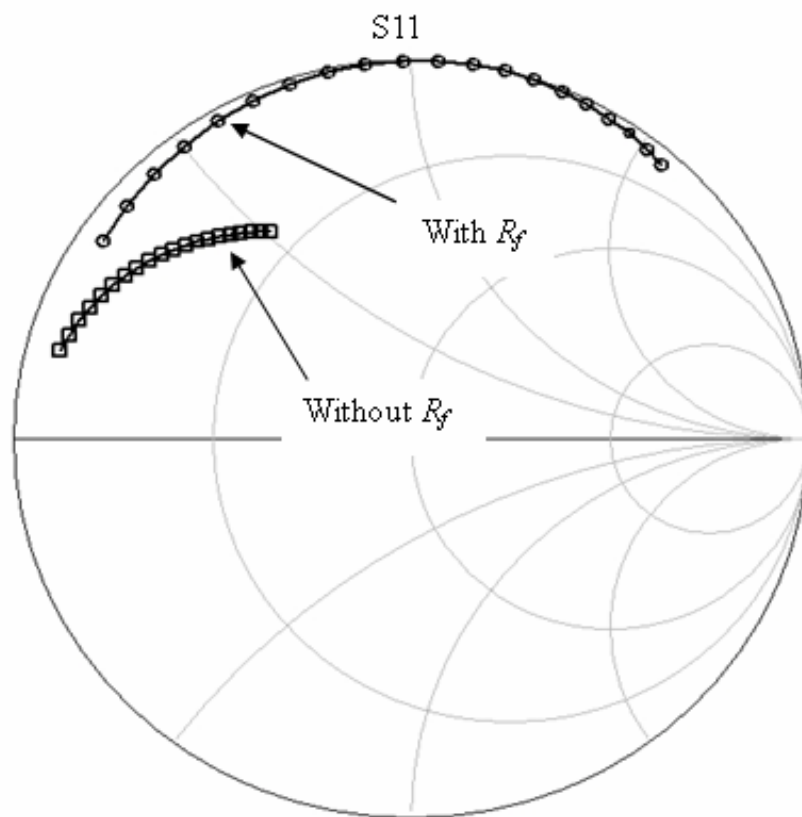
Fig. 4.31 S11 of the proposed active inductor

4.4.2 Simulation Results

All simulations are implemented via an Aligent-ADS simulator. The active devices are modeled by TSMC 0.25um CMOS process at 2.5V. All transistors have the same dimensions, and the length and width of each MOSFET are 0.24 um and 40 um respectively. The feedback resistance is chosen to be $R_f = 2K\Omega$. As a result, the scattering parameter S11 performance of the active inductor is shown in Fig. 4.31. It can be seen that between 0.5GHz and 2.5GHz, the curve is inclined to the outside of the circle, indicating that the loss is decreased. Thus, the Q-value is significantly improved.

Figs. 4.32, 4.33, and 4.34 show the Q-value, inductance and the equivalent loss comparisons between the active inductor with feedback resistor R_f and the one without it. Figure 4.32 and 4.34 indicate that in the range of 0.5GHz to 2.5GHz, the maximum Q-value is around 1E8 and the inductance changes from 5nH to 7.5nH. The Q-value and the inductance of the active inductor with feedback resistor are higher than that of the one without it. Fig. 4.34 shows the minimum equivalent loss of a proposed active inductor with feedback resistor is 1.2E-8Ω and it is much smaller than that of the one without the feedback resistor between the frequency ranges of 0.5GHz and 2.5GHz. Consequently, the active inductor has shown a significant improvement. The power consumption is only about 2.5mW under 2.5 V supply voltage, and there is lesser power consumption in this active inductor. Furthermore, in this active inductor, the external bias voltages are used to tune the characteristics of the active inductor due to th e variation in the circuit implementation. Therefore, it can be achieved the performances that independent of the process variation. The proposed active inductor layout is showed in Fig. 4.35. The size of the chip is about 1053um × 713um. The comparisons between improved and original at 1.5GHz is shown in TABLE 4.4.
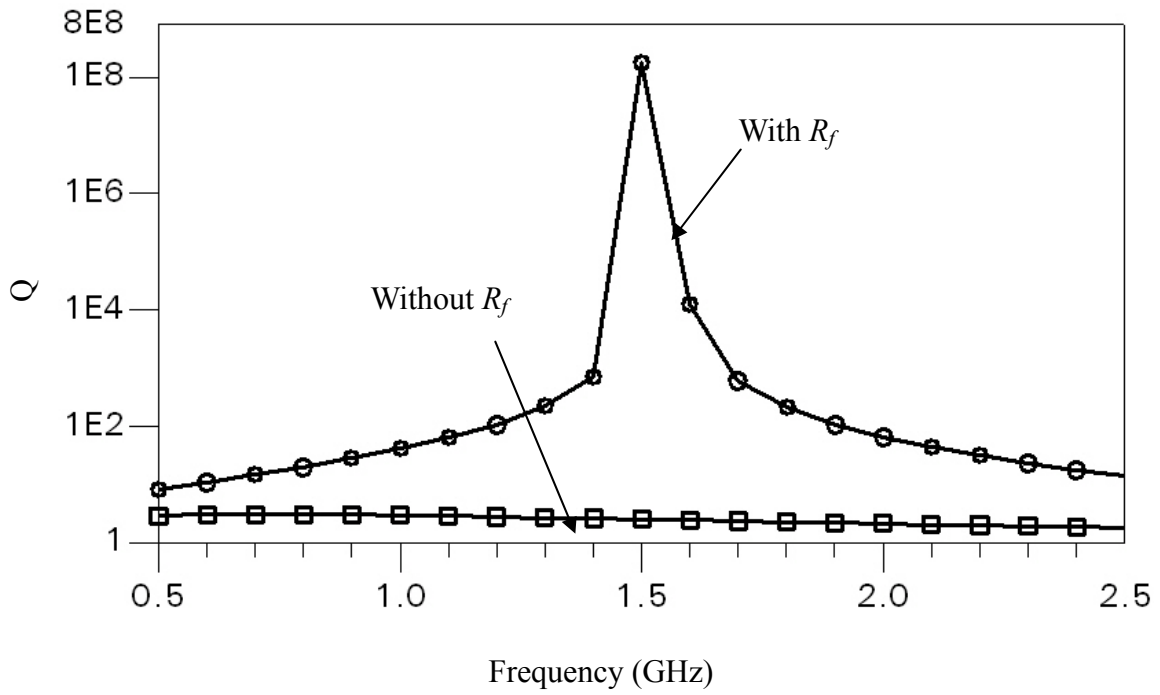
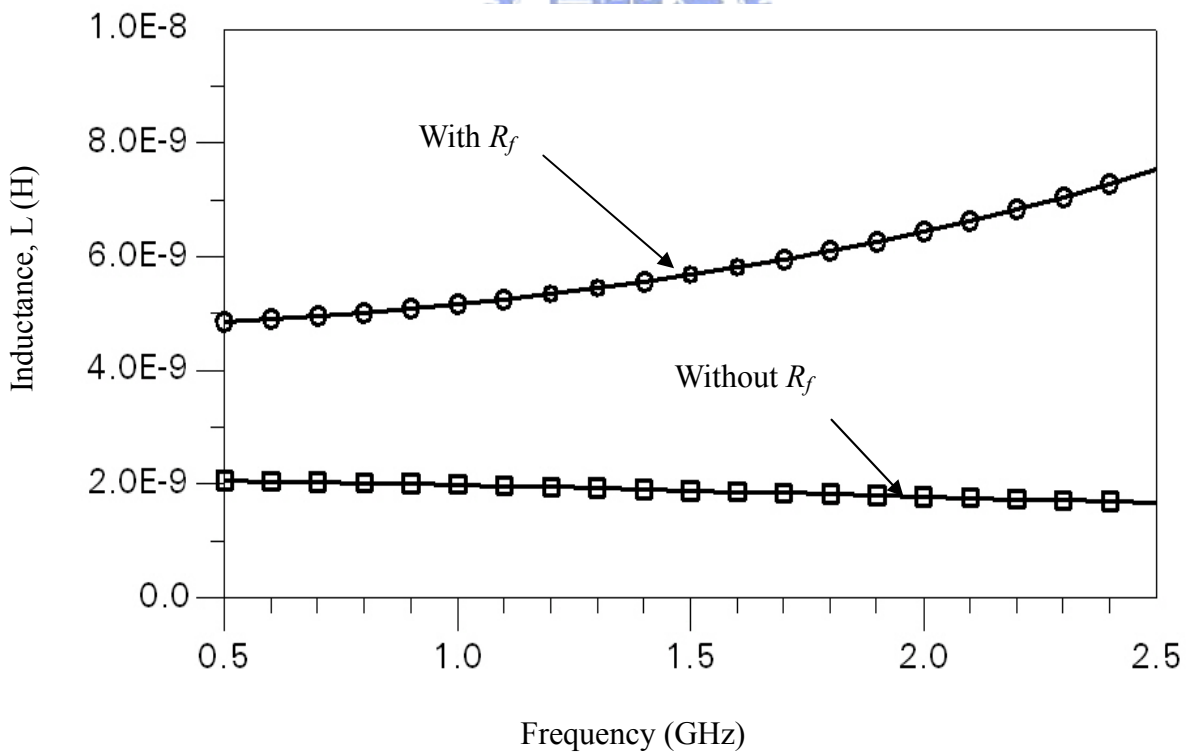Fig. 4.32 Q-value of the proposed active inductor circuit

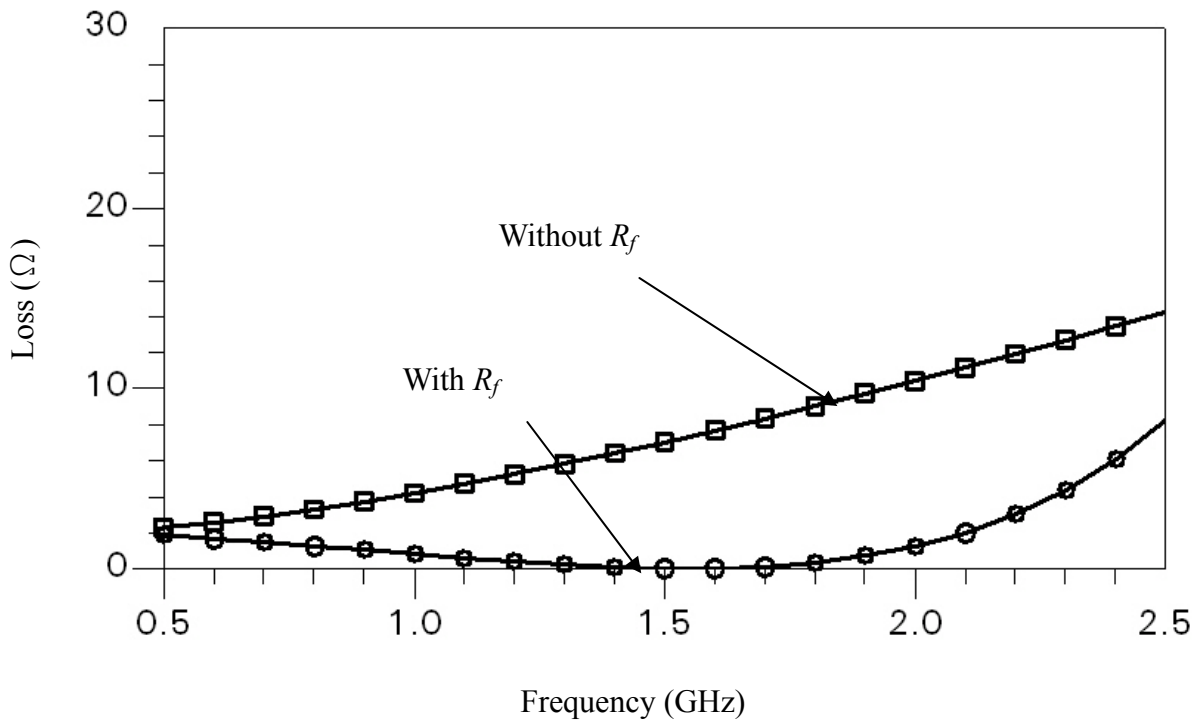Fig. 4.33 Inductance of the proposed active inductor circuit

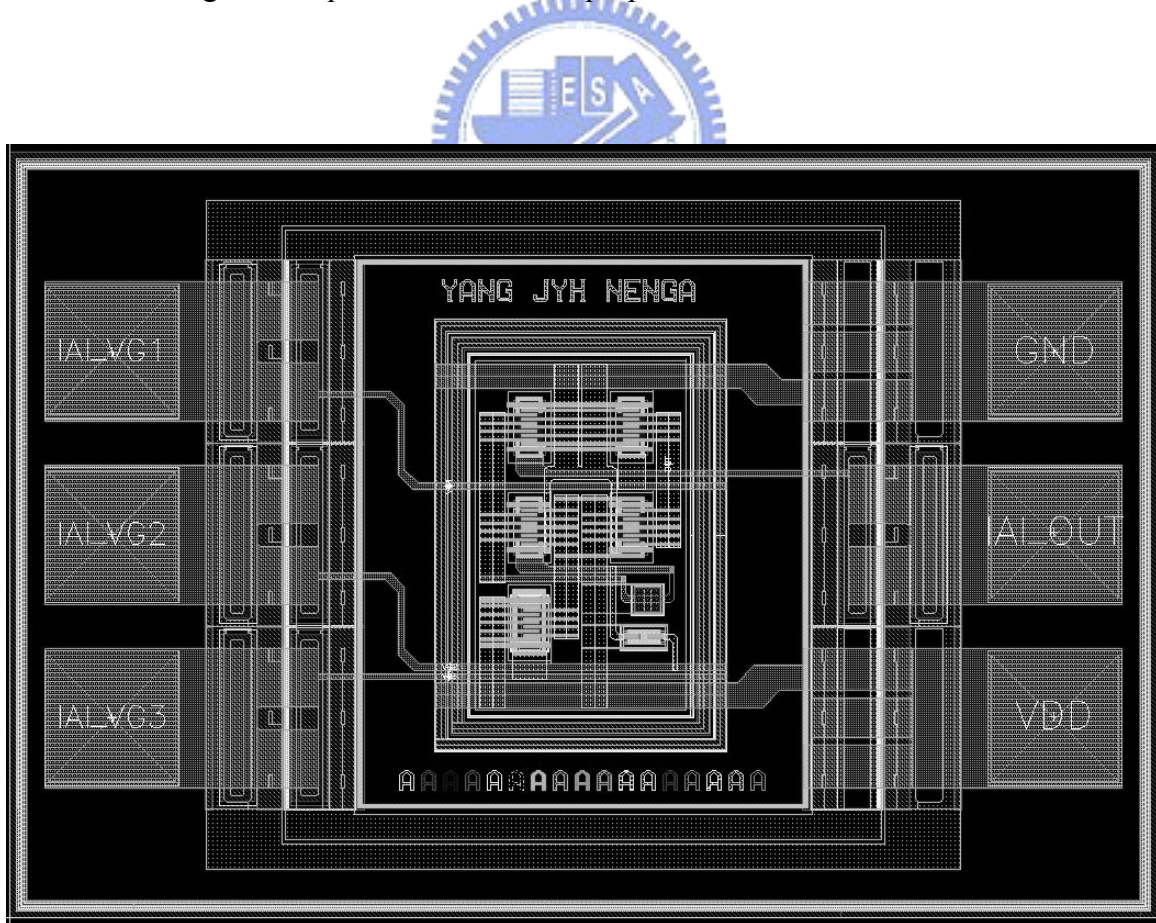Fig. 4.34 Equivalent loss of the proposed active inductor circuit

Fig. 4.35 Layout of the proposed active inductor circuit

TABLE 4.5 COMPARISONS BETWEEN IMPROVED AND ORIGINAL @1.5GHZ

	Improved	Original
Q	1E8	1.4
Loss (Ohm)	1.2E-8	8
Inductance (H)	5.8n	2
Power Consumption (mW)	2.5	3

4.4.3 Discussion

A CMOS high-Q RF active inductor using a simple loss compensation circuit is proposed. Only one resistor is added to the feedback loop to compensate the loss of CMOS active devices and the external bias voltage is used to compensate the variation in IC fabrication. As a result, in the 0.5GHz to 2.5GHz frequency range, a higher Q-value, inductance value, and reasonable power consumption under 2.5V voltage supplies voltage are achieved. Simulation results show that the proposal achieves better performance indices when comparing to the original active inductor published earlier. In consequence, a significant improvement in Q-value and inductance is achieved with relative low power consumption.

4.5 Summary

In this chapter, the improved active inductors using various compensation techniques for improving the performance of the active inductor are presented. The proposed loss compensation techniques, which use only a simple RC feedback network, current-reused and gain boosting technique, a capacitor, and a resistor to significantly increase the Q-value, the inductance, and the operating frequency. The power consumption of the improved active inductor can be obviously reduced by using the loss compensation techniques. Furthermore, the circuit of the improved active inductor is very simple. In additional, the size of the improved active inductor is smaller than that of the planar spiral inductor.

Chapter 5

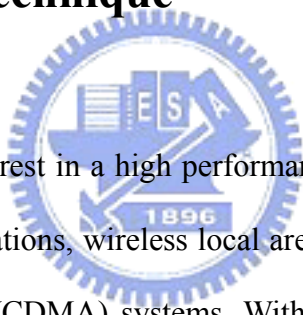# Applications Based on Improved CMOS Active Inductors

Most of the previous reports in CMOS wideband amplifier applications are implemented by using chip passive spiral inductors or resistors to achieve better matching, wider bandwidth, and higher power gain [47]-[52]. The CMOS voltage controlled oscillators are also implemented by using chip passive spiral inductors to obtain required output voltage, good phase noise, and high tuning range [53]-[55]. However, the low quality factor (Q value) and the large chip size of an integrated passive inductor cause the decreasing of the circuit performance. In addition, a high performance wideband amplifier and voltage-controlled oscillator require a larger load resistance or a higher quality inductance. Then the size of the chip and the cost of the large load resistance and the higher quality inductance can be significantly increased. Therefore, to design a RF integrated circuit for achieving required performances, a high quality factor inductor and a small chip area inductor are necessary. To solve these problems, an active inductor is an alternate approach to design the circuits.

In this chapter, a wide-band amplifier and a voltage-controlled oscillator based on an active inductor are presented. The wide-band amplifier and the voltage-controlled oscillator are used to improve high-Q active inductor for achieving high gain-bandwidth, a reasonable

performance and small chip size. The organization of this chapter is as the following. In section 5.1, a CMOS wide-band amplifier based on the improving high-Q active inductor, which uses a loss compensation technique of the cascode RC feedback, is presented. In section 5.2, a CMOS LC oscillator using a high-Q active inductor based on a feedback resistor of loss compensated technique is described. Finally, a brief summary is made in section 5.3.

5.1 Wideband Amplifier Based on Improved Active Inductor Using a Cascode RC Feedback Compensation Technique

There is a considerable interest in a high performance, low power wideband amplifier for multi-band mobile communications, wireless local area network (WLAN), and wideband code division multiple access (WCDMA) systems. With the advent of high speed, narrow gate-length CMOS process becoming commercially available and abundant recently, the potential for high levels of CMOS wideband amplifier are also becoming realizable.

In Most of the previous reports of CMOS wideband amplifier applications, the load and the matching network are implemented by using on chip passive spiral inductors or resistors to achieve high power gain, good matching, and wide bandwidth [47]-[49]. To obtain a high performance wideband amplifier, a higher quality inductance or a larger load resistance is required. However, the high quality factor of an integrated passive inductor is substantial low, and the performances of the wide bandwidth will be significantly degraded. Moreover, a high quality of spiral inductor and a larger load resistance often require additional processing steps to compensate the quality factor and a larger chip size, and an extra cost for achieving this

goal is also required [50]. Furthermore, the inductance of the CMOS passive inductor is dependent on the chip size [25]. Therefore, the chip size of an integrated passive spiral inductor is usually larger when it is compared to other components of CMOS IC, and it also limits the wideband amplifier performance. The above difficulties can be overcome by using a CMOS active inductor.

In this work, we design an integrated CMOS wideband amplifier based on a low loss active inductor with 0.25um standard CMOS process. This active inductor improves not only the performance of the passive spiral inductor and conventional cascode active inductor (e.g. Q value, inductance, and operating frequency), but also the wideband amplifier performance. This design can be competed with the one using a passive spiral inductor and a conventional cascode active inductor.

In order to achieve larger power gain and wider bandwidth of a wideband amplifier, the multi-stage amplified circuit, low loss inductive load, and negative feedback configuration techniques are simultaneously used. A wideband amplifier with active inductor load can meet the above requirements and obtain the expecting performance.

The organization of this section is as the following. The wideband amplifier based on the conventional cascode active inductor is expressed in section 5.1.1. The design of the improved high-Q active inductor circuit is described in section 5.1.2. The wideband amplifier based on the improved high-Q active inductor is expressed in section 5.1.3. The simulation results of the wideband amplifier based on the improved high-Q active inductor are depicted in section 5.1.4. The measured results of the wideband amplifier based on the improved high-Q active inductor are displayed in section 5.1.5. Finally, the discussion is given in section 5.1.6.

5.1.1 Wideband Amplifier with Conventional Cascode Active Inductor

According to Fig. 5.1, a negative feedback loop of the gyrator configuration is constructed by the transconductance $-G_{m1}$ and G_{m2}. A wideband amplifier with gyrator configuration can be designed as Fig. 5.2. The close loop gain of the gyrator amplifier is expressed as Eq. (5.1).
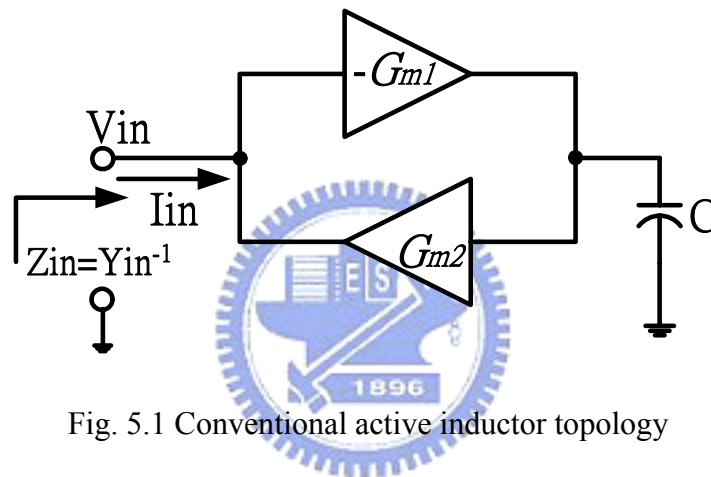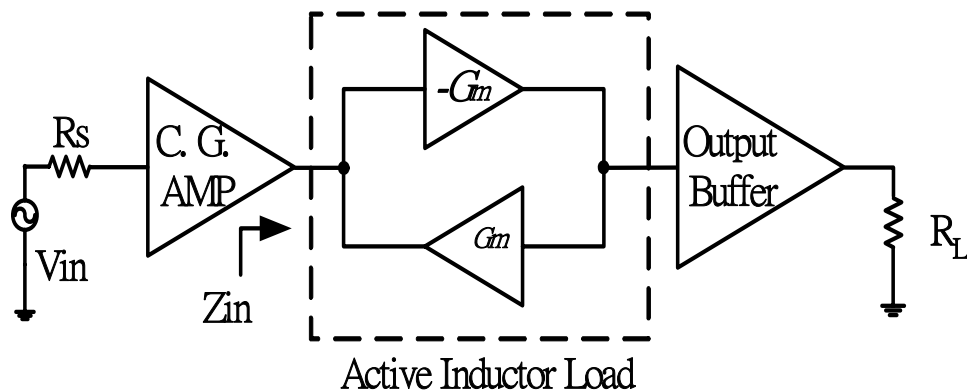
Fig. 5.1 Conventional active inductor topology

Fig. 5.2 The wideband amplifier using active inductor configuration

$$Av = \frac{V_{out}}{V_{in}} = \frac{-G_{m1}}{1 + G_{m1}G_{m2}} \tag{5.1}$$

From Fig. 5.2, the wideband amplifier configuration is comprised of four function blocks, which are the input stage, the active inductor stage, the negative feedback function, and the output buffer stage, to achieve the high gain and the wide bandwidth.

An overall voltage gain ($A_{v,overall}$) of the CMOS wideband amplifier based on the active inductor configuration can be expressed as Eq. (5.2).

$$A_{v,overall} = A_{v,C.G.} \times A_{v,active\_inductor} \times A_{v,buffer}$$

$$= G_{m,C.G.} \times Z_{in} \times \frac{-G_{m1}}{1+G_{m1}G_{m2}} \times A_{v,buffer} \tag{5.2}$$

where $A_{v,C.G}$ and $G_{m,C.G.}$ are the voltage gain and the transconductance of the common gate amplifier, respectively. $A_{v,buffer}$ is the gain of the buffer stage. From Eq. (5.2), the load impedance ($Z_{in}=Y_{in}^{-1}$) of the wideband amplifier will affect its overall voltage gain. The high load impedance will increase the overall voltage gain of the wideband amplifier, and the lower loss of the active inductor will increase the higher overall voltage gain of the wideband amplifier.
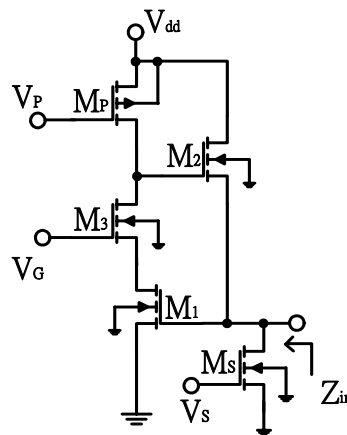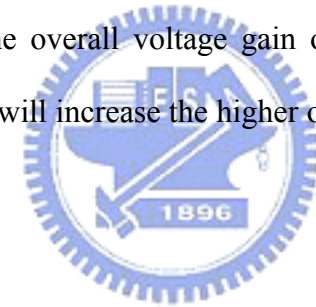

Fig. 5.3 A conventional cascode active inductor circuit

Based on the wideband amplifier topology, a convention cadcode active inductor, shown as Fig. 5.2, is applied in the CMOS wideband amplifier topology and is shown in Fig.

5.3. A cascode active inductor of the CMOS wideband amplifier comprises with transistors M_1, M_2, M_3, and Mp. The cascode active inductor connects between the common gate amplifier and the output buffer stage to act as the load of the common gate amplifier. The common gate amplifier is constructed by M_{S1} and M_{S2} to achieve the higher linearity and the higher isolation. Transistor M_B and resistor R_B composes the output buffer stage. The output buffer produces higher output current and lower output impedance to drive the low output load ($50\,\Omega$) and to achieve good matching. The overall voltage gain of this wideband amplifier can be expressed as Eq. (5.3).
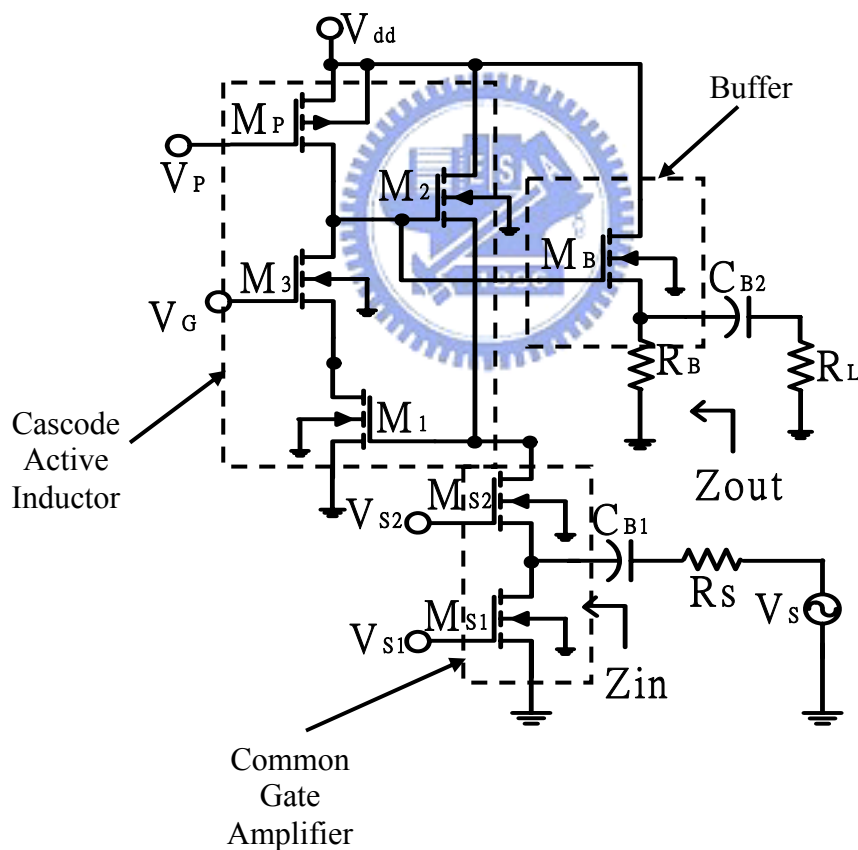

Fig. 5.4 Wideband amplifier circuit based on conventional active inductor

$$A_{v,overall} = A_{v,C.G.} \times A_{v,activeinductor} \times A_{v,buffer}$$

$$\approx A_{v,C.G.} \times [(g_{dsp} + g_{mp} + g_{ds1}) + sC_{gs1} + \frac{g_{m1}g_{m2}g_{m3}}{(sC_{gs2}+g_{ds1}g_{ds3})})^{-1}]$$

$$\times(\frac{g_{m1}g_{m3}}{C_{gd1}g_{ds3}} \frac{\frac{sC_{gs2}(sC_{gd1}+g_{m3})}{g_{m1}g_{m3}}-1}{s+\frac{sC_{gs2}(sC_{gd1}+g_{m3})}{C_{gd1}g_{ds1}}}) \times A_{v,bufer}$$

(5.3)

where g_{mi} is the transconductance of transistor; C_{gsi} and C_{gdi} are the capacitance of gate to source and the capacitance of gate to drain, respectively; g_{dsi} is the conductance of the MOSFET. From the Eq. (5.3), owing to the loss of the active inductor, the Q-value of the active inductor will be decreased. Thus, the lower Q value of the active inductor load will degrade the bandwidth of the wideband amplifier. Furthermore, the lower Q-value will reduce the load impedance of the common gate amplifier operating in higher frequency. Therefore, the bandwidth of the common gate amplifier will be limited by the loss of the active inductor in higher operating frequency.

The simulation results of the wideband amplifier are shown in Fig. 5.4 and these results indicates that the S-parameter values are 25dB of S21, -16dB of S11, -25dB of S22, and -80dB of S12, respectively. Although the gain (S21) can achieve 25dB, the bandwidth is relatively narrow and is about 0.3GHz. Figure 5.5 shows the 8.2dB noise figure within 3GHz frequency. The noise figure can obtain flat response within the wide frequency range. Fig. 5.6 and 5.7 indicate the results of the linearity of the wideband amplifier. The 1 dB compression and the IIP3 are about –28dBm and –14dBm, respectively. From the simulation results, the bandwidth of the amplifier is significantly narrow. To improve the bandwidth of the amplifier, the loss of active inductor load should be decreased. The loss of the active inductor is reduced; the load impedance of the common gate amplifier will be increased. The bandwidth of the amplifier will be expanded. Therefore, the improved active inductor, which uses the cascode

RC feedback configuration to compensate the loss of the active inductor, acts as the load of the common gate amplifier to improve the operating bandwidth of the wideband amplifier.
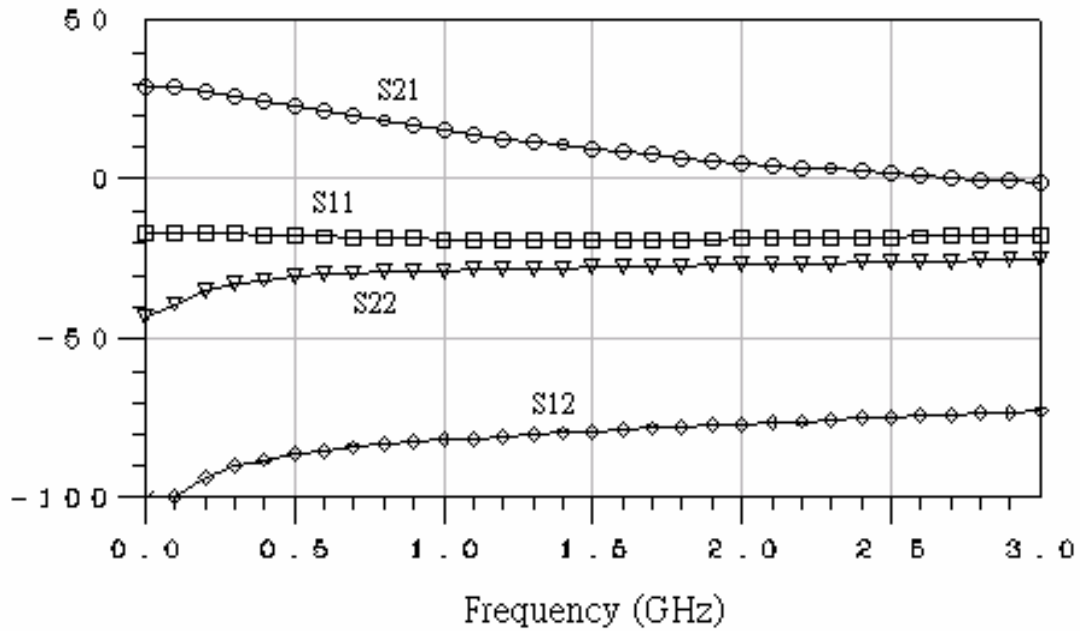

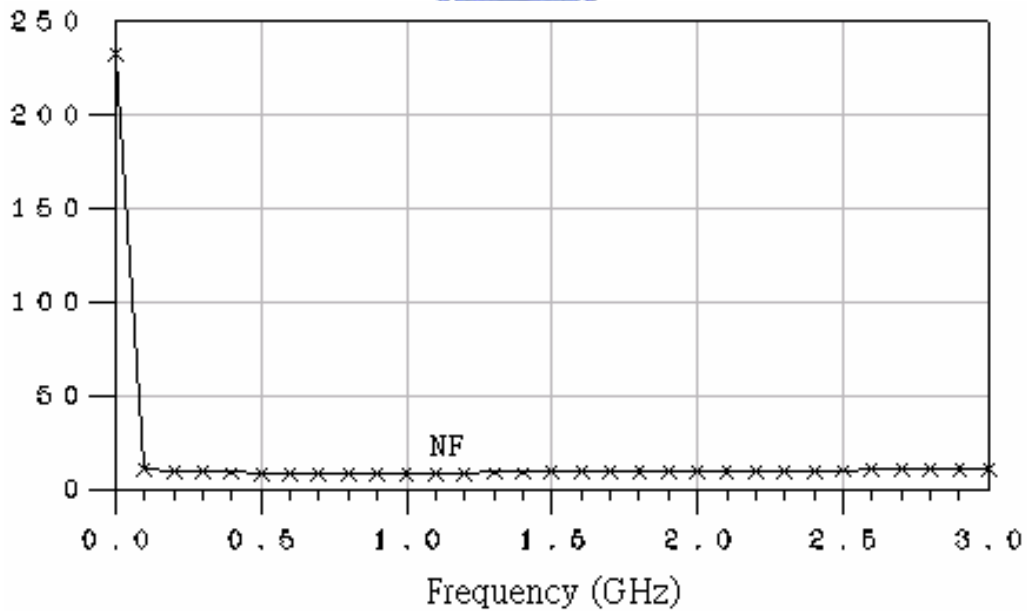Fig. 5.5 S-parameters of the wideband amplifier based on conventional active inductor

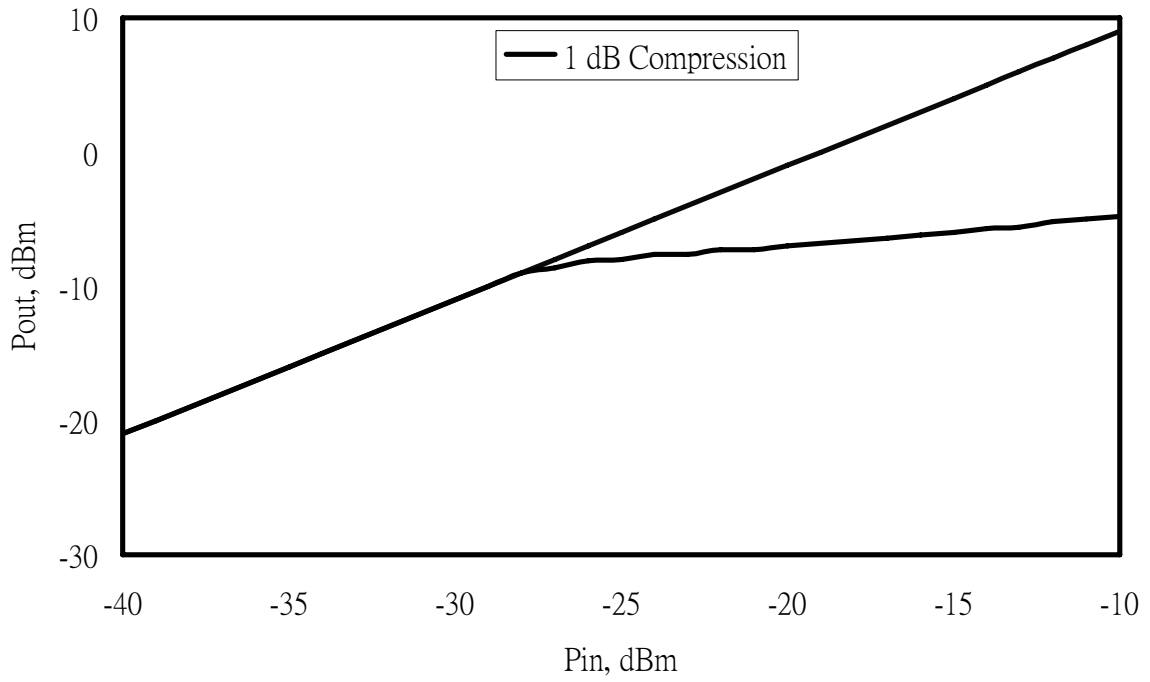Fig. 5.6 Noise figure of the wideband amplifier based on conventional active inductor

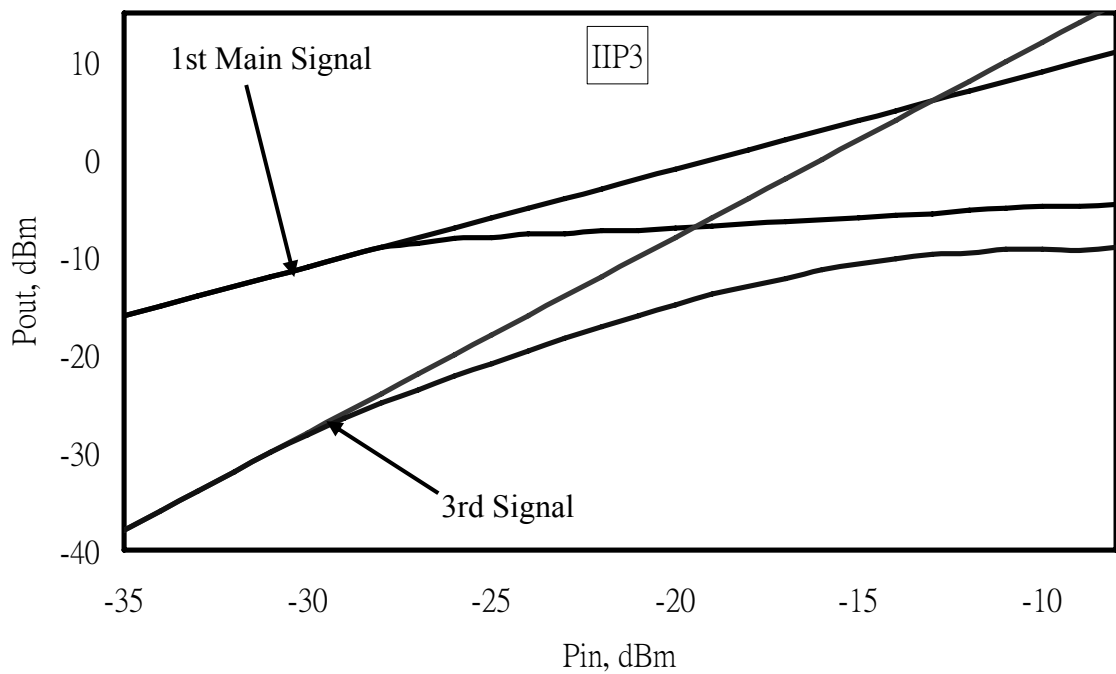Fig. 5.7 1dB compression of the wideband amplifier based on conventional active inductor

Fig. 5.8 IIP3 of the wideband amplifier based on conventional active inductor

5.1.2 Improved High-Q Active Inductor Design

A conventional active inductor is designed by the combination of a gyrator where two transconductors are connected in back-to-back configuration and a capacitor [34]. The typical gyrator topology, showed in Fig. 5.1, includes the functions of the inductive impedance and negative feedback amplifier, where G_{m1} and G_{m2} are the transconductance of feedback amplifier.

Using the topology of Fig. 5.1, the conventional cascode active inductor circuit is shown in Fig. 5.2 and the equivalent input impedance is expressed as Eq. (5.4).

$$Z_{in} = Y_{in}^{-1} \approx [(g_{dsp} + g_{mp} + g_{ds1}) + sC_{gs1} + \frac{g_{m1}g_{m2}g_{m3}}{sC_{gs2} + g_{ds1}g_{ds3}}]^{-1} \qquad (5.4)$$

From Eq. (5.4), the impedance loss of $(g_{dsp} + g_{mp} + g_{ds1})$ and $\dfrac{g_{m1}g_{m2}g_{m3}}{g_{ds1}g_{ds3}}$ reduce the performance of the active inductor. In order to improve the performance of the active inductor, an improved active inductor circuit, which shown in Fig. 5.9, is proposed. The improved active inductor includes a simple RC feedback network for compensating the impedance loss. The loss is caused by the conductance between drain and source of MOSFETs.

In Fig. 5.9, the C_N, R_G and M_3 construct a common gate configuration in the positive feedback path, and the configuration has a negative conductance, which compensates the loss, $(g_{dsp} + g_{mp} + g_{ds1})$ and $\dfrac{g_{m1}g_{m2}g_{m3}}{g_{ds1}g_{ds3}}$, of the active inductor expressed in Eq. (5.4). The negative conductance G_N is generated by C_N, R_G and M_3, which are also interacting with M_1 and M_2. Thus, G_N can be derived as Eq. (5.5).
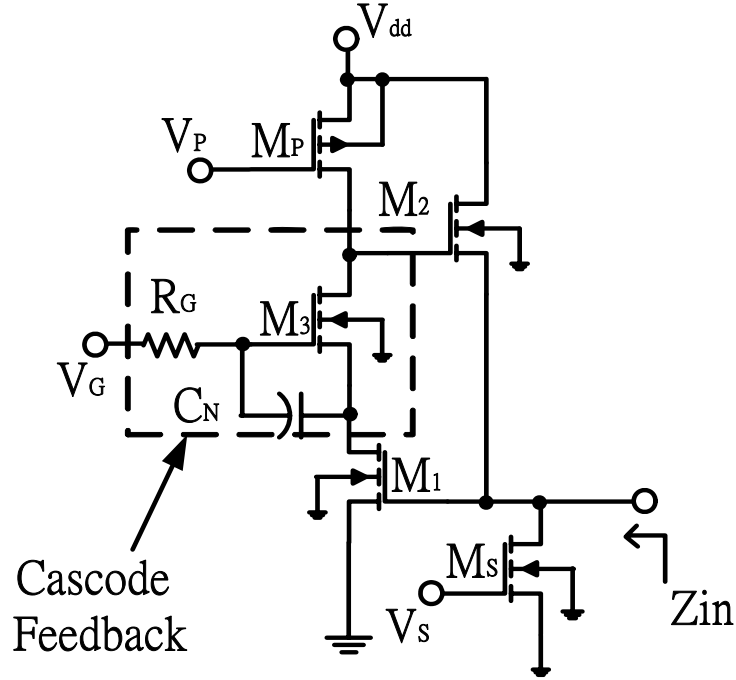
Fig. 5.9 Improved active inductor circuit

$$G_N \approx -\frac{(g_{m1}g_{m3}/g_{dsp}) + g_{m3} + sC_N}{g_{m3} + sC_N} g_{m2} \qquad (5.5)$$

Then the equivalent input impedance of the improved active inductor can be approximated as Eq. (5.6).

$$Z_{in} = Y_{in}^{-1} \approx [(g_{dsp} + g_{mp} + g_{ds1}) + sC_{gs1}$$
$$+ \frac{g_{m1}g_{m2}g_{m3}}{sC_{gs2} + g_{ds1}g_{ds3}} - \frac{(g_{m1}g_{m2}/g_{dsp}) + g_{m3} + sC_N}{g_{m3} + sC_N} g_{m2}]^{-1} \qquad (5.6)$$

From Eq. (5.6), if the circuit components and biases are properly chosen, the input impedance loss could be reduced by the minus term in Eq. (5.5), and the performance of active inductor can be improved. The comparison between the scattering parameter S_{11} of the improved active inductor and the conventional cascode active inductor with the same 0.25 um TSMC process is shown in Fig. 5.10. In Fig. 5.10, the curve of the improved active inductor

is inclined outer than that of the curve of the conventional cascode active inductor between 0.8GHz and 3GHz, and the loss is also decreased. This effect will improve the Q-value apparently. Furthermore, the curve of the improved active inductor shifts to tend right, which indicates that the improved active inductor has higher inductance and operating frequency than that of the conventional coscode active inductor.
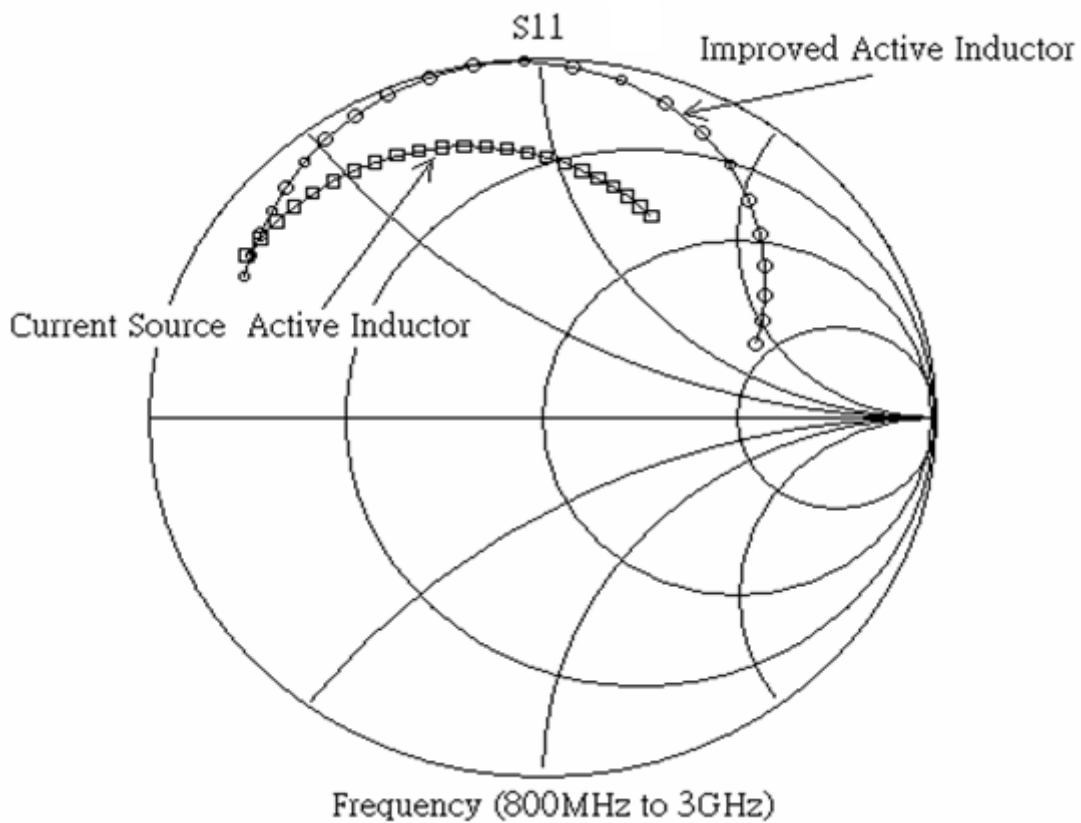

Fig. 5.10 S11 parameter of active inductors

Because the Q value, inductance, and the operating frequency of the improved active inductor are significantly improved, the improved active inductor can be used to design the wideband amplifier. The performance of the wideband amplifier based on the improved active inductor is greatly promoted.

5.1.3 Wideband Amplifier with Improved Active Inductor

In order to improve the bandwidth, a CMOS wideband amplifier based on the improved active inductor is designed. The wideband amplifier also consists of three stages, which includes the common gate amplifier, the low loss improved active inductor, and the buffer stage, is shown as Fig. 5.11. The common gate amplifier stage is comprised of M_{S1} and M_{S2}. It provides low input impedance (about $1/g_{ms2}$) for matching 50Ω source impedance, higher linearity amplification and effective reverse isolation with impedance. The input impedance can be expressed as Eq. (5.7).

$$Z_{in} \approx \frac{1}{g_{ms\,2}} // \frac{1}{g_{dss\,1}} // \frac{1}{g_{dss\,2}} \approx \frac{1}{g_{ms\,2}} \qquad (5.7)$$

The low loss high-Q novel active inductor is constructed by $M_1 \sim M_3$ and M_P transistors, resistor R_G, and capacitor C_N to configure as the load of the common gate amplifier for higher gain and wider bandwidth. Transistor M_B and R_B construct the output buffer stage. The output buffer stage is a common drain configuration, which provides a minimized loading effect of a 50Ω output impedance matching. C_{B1} and C_{B2} are DC blocking capacitors of the input and output to isolate the DC bias between the previous stage and the next stage. Therefore, the overall gain of the wideband amplifier can be expressed as Eq. (5.2), and is rewritten as below.

$$A_{v,overall} = A_{v,C.G.} \times A_{v,activeindu\,ctor} \times A_{v,buffer}$$

Because the improved active inductor is used in the CMOS wideband amplifier, the load impedance of the common gate amplifier can be written as Eq. (5.6). In consequence, the overall gain of the wideband amplifier based on the improved active inductor is changed to Eq. (5.8).

$$A_{v,overall} \approx A_{v,C.G.} \times [(g_{dsp} + g_{mp} + g_{ds1}) + sC_{gs1} + \frac{g_{m1}g_{m2}g_{m3}}{(sC_{gs2}+g_{ds1}g_{ds3})}$$

$$- \frac{g_{m1}g_{m2}/g_{dsp}+g_{m3}+sC_N}{g_{m3}+sC_N} g_{m2})^{-1}] \times (\frac{C_N g_{m1}g_{m3}}{C_{gd1}g_{d3}} \frac{\frac{sC_{gs2}(sC_{gd1}+g_{m3})}{g_{m1}g_{m3}}-1}{s+\frac{sC_{gs2}(sC_{gd1}+g_{m3})}{C_{gd1}g_{ds1}}}) \times A_{v,bufer} \qquad (5.8)$$
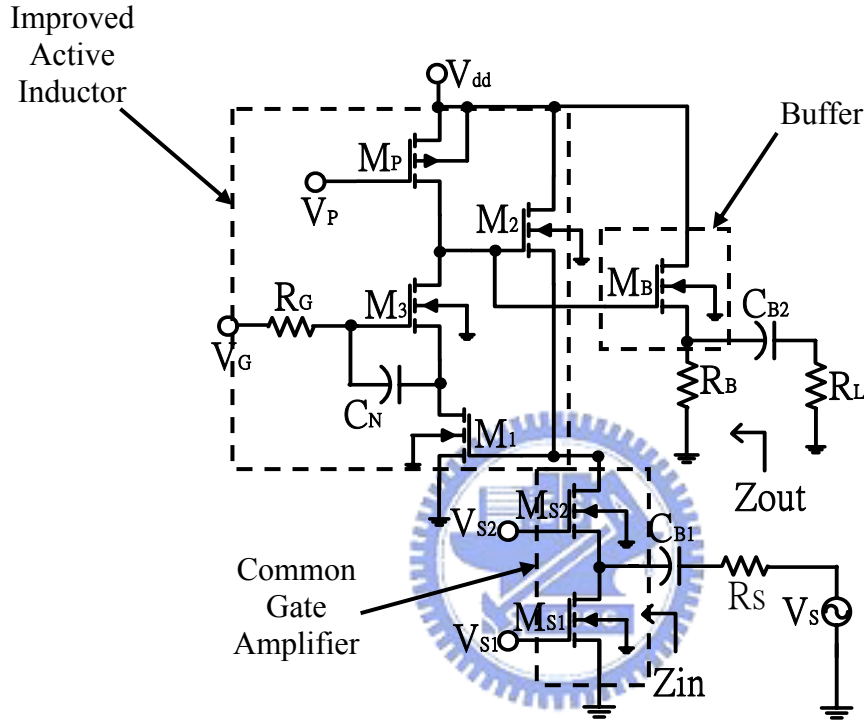

Fig. 5.11 Wideband amplifier circuit based on improved active inductor

From Eq. (5.8), the equivalent losses of Z_{in} (Y_{in}^{-1}) are reduced and the Q value of the inductor is increased. As a result, the load impedance of the common gate stage is raised. In addition, the inductance and the operating frequency are significantly improved, and the operating frequency of the amplifier can be expanded. Thus, the overall gain is also improved significantly. Consequently, the performance of the wideband amplifier is improved apparently by using the improved active inductor. Furthermore, the CMOS wideband amplifier can modify the overall circuit response by tuning the biases of V_{S1}, V_{S2}, V_G and V_P.

5.1.4 Simulation Results

The CMOS wideband amplifier based on the conventional cascode active inductor and the improved active inductor in TSMC 0.25 um CMOS process technology was simulated by using Agilent ADS simulator. In Fig. 5.3 and 5.10, all transistors use the same dimensions (W=0.24um and L=40um) and model.

The simulated characteristics of the wideband amplifier based on the conventional cascode active inductor are displayed in previous section. The wideband amplifier based on improved active inductor was simulated in $V_{S1}=V_{S2}=1V$, $V_G=1.7V$, $V_P=1.4V$ bias voltages, and provided 2.5V normal supply voltage. The simulated results of S-parameters are shown from Fig. 5.12 to Fig. 5.15. Figure 5.12 shows the S-parameters. The forward power gain S21 is about 21dB, and the input reflection coefficient and output reflection coefficient S11, S22 are –17dB and –21dB, respectively. The reverse transmission S12 is lower than –65 dB. From the curve of the S21, the response is nearly flat from 0Hz to 1.3 GHz. By the definition of –3dB (three dB cutoff) frequency response, the bandwidth of the wideband amplifier has 1.3GHz bandwidth. The power consumption is about 18mW. Figure 5.13 shows the noise figure (NF) of the CMOS wideband amplifier based on the improved active inductor and this noise figure is about 8dB in the range of 0.1GHz to 3 GHz. The noise figure is also independent of the frequency. Fig. 5.14 and 5.15 indicate the results of the linearity of the wideband amplifier. The 1 dB compression and the IIP3 are about –16dBm and –13dBm, respectively..

The comparison of the wideband amplifier based on the improved active inductor load to the conventional cascode active inductor load is summered in TABLE 5.1. The forward gain S21 of the wideband amplifier based on the conventional cascode active inductor load is decayed rapidly due to the high loss of the active inductor, and its bandwidth is only 0.3GHz. The wideband amplifier based on improved active inductor load has remained forward gain

to 1.3GHz. The bandwidth is wider than that of the one using the conventional cascode active inductor load. In addition, the Q-value of the improved active inductor is higher than the Q-value of cascode active inductor. The power consumption of the wideband amplifier using an improved active inductor has only consumed 18mW, but the power consumption of the one using the conventional cascode active inductor wideband amplifier requires 30 mW for the same gain. For the matching characteristics, the improved active inductor will bring the reversed transmission isolation S12 and output matching S22 characteristics a little decayed, but it still meets the requirement in many applications. For the noise figure, two amplifiers have similar results when acting as the cascode active inductor wideband amplifier. For the linearity, the wideband amplifier based on the improved active inductor is better than that of the wideband amplifier using the conventional cascode active inductor.

TABLE 5.1
COMPARISON OF WIDEBAND AMPLIFIERS BASED ON TWO DIFFERENT ACTIVE INDUCTORS

Active inductor	S_{21} (dB)	S_{11} (dB)	S_{22} (dB)	S_{12} (dB)	Bandwidth (GHz)	Noise Figure (dB)	Power Dissipation (mW)
Conventional	25	-16	-25	-80	0.3	8.2	30
Improved	21	-17	-21	-65	1.3	8	18

In this work, there are some competitive performances in CMOS wideband amplifier. The comparison between the CMOS wideband amplifier based on the improved active load and the other published works [47, 49] and [51, 52] is also shown in TABLE 5.2. From the comparison, our work is superior to those wideband amplifiers in some features. The layout of the proposed wide-band amplifier is displayed in Fig. 5.16. The size of the wide-band amplifier is about 866um $\times$ 824um.
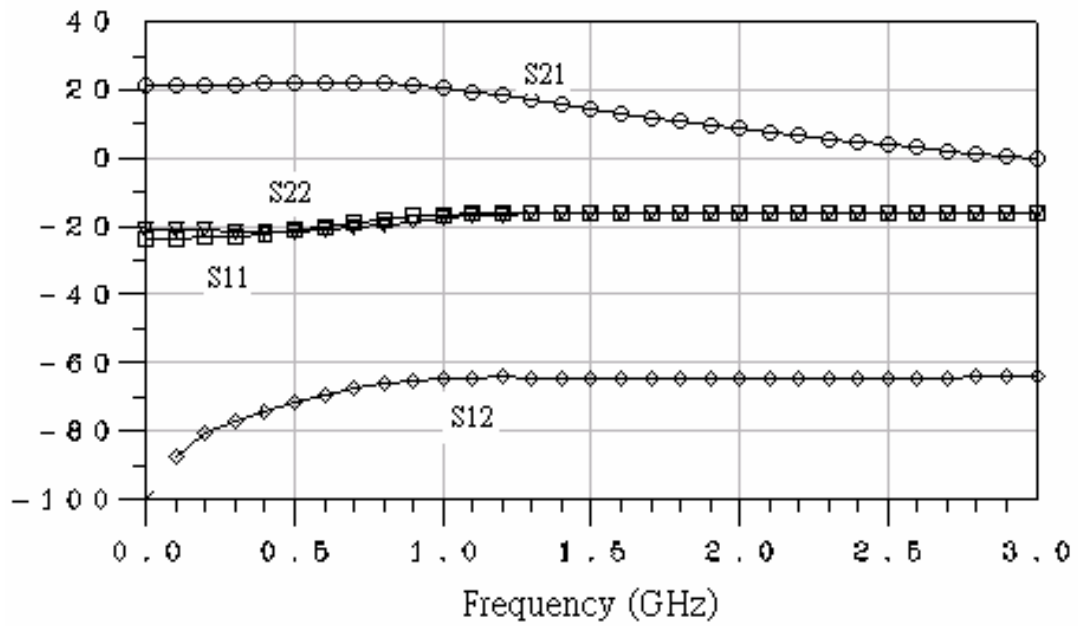
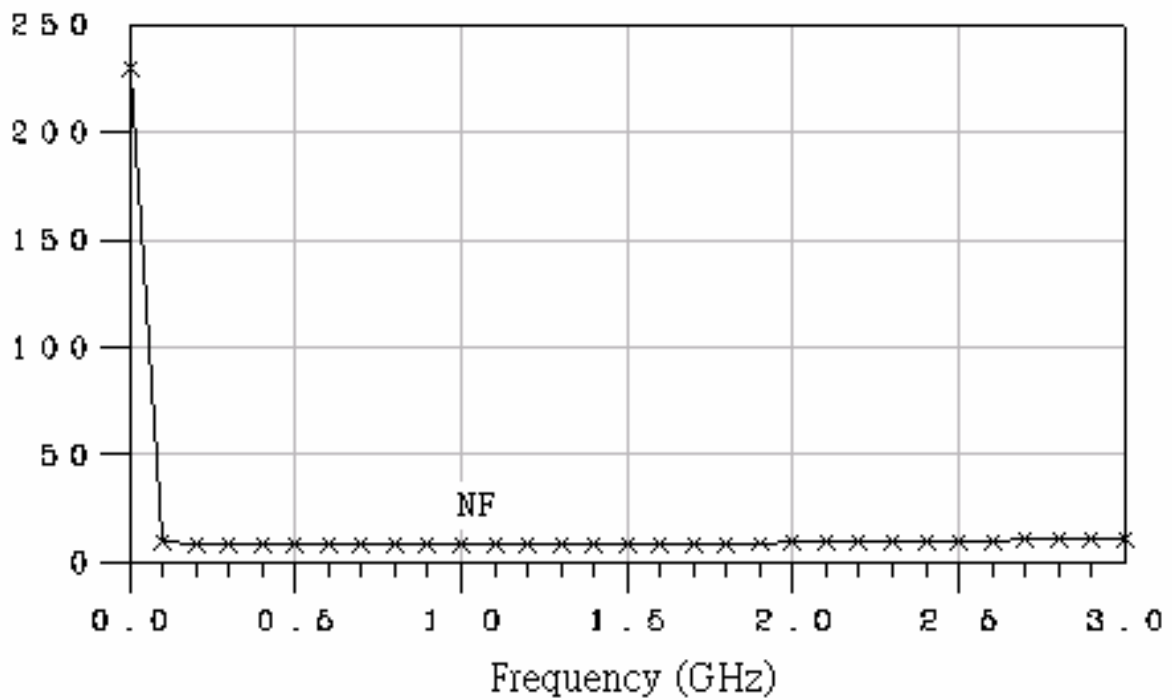Fig. 5.12 S-parameters of wideband amplifier based on novel active inductor

Fig. 5.13 Noise figure of wideband amplifier based on novel active inductor
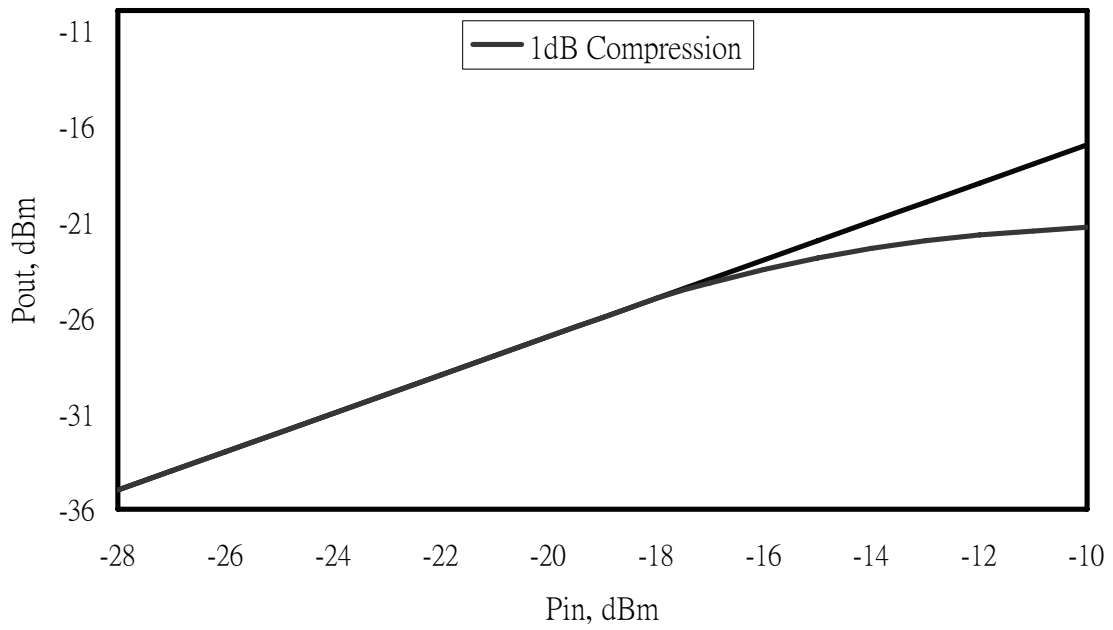
Fig. 5.14 1dB compression of wideband amplifier based on novel active inductor
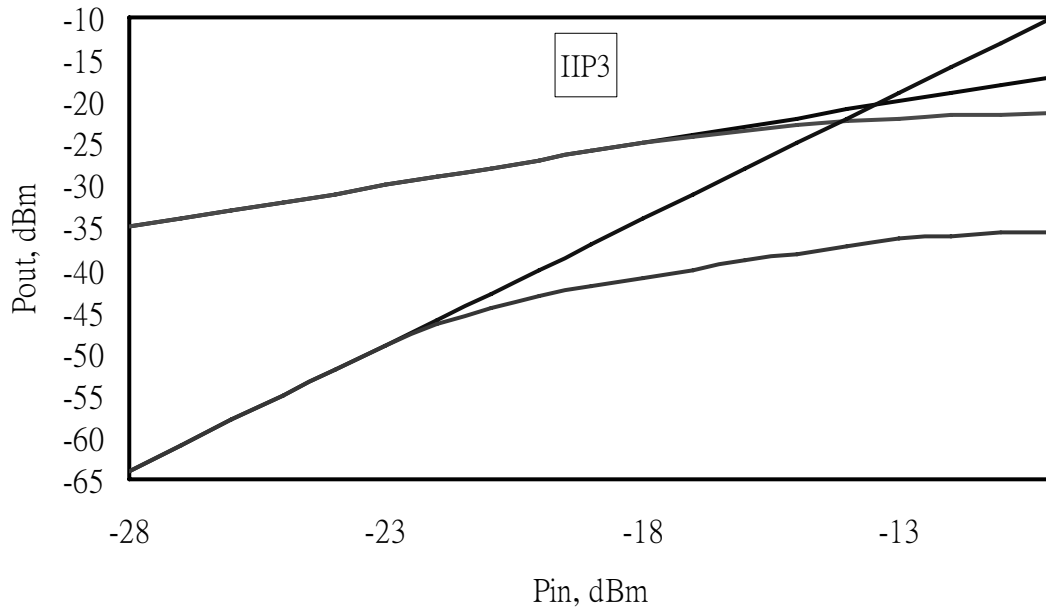

Fig. 5.15 IIP3 of wideband amplifier based on novel active inductor
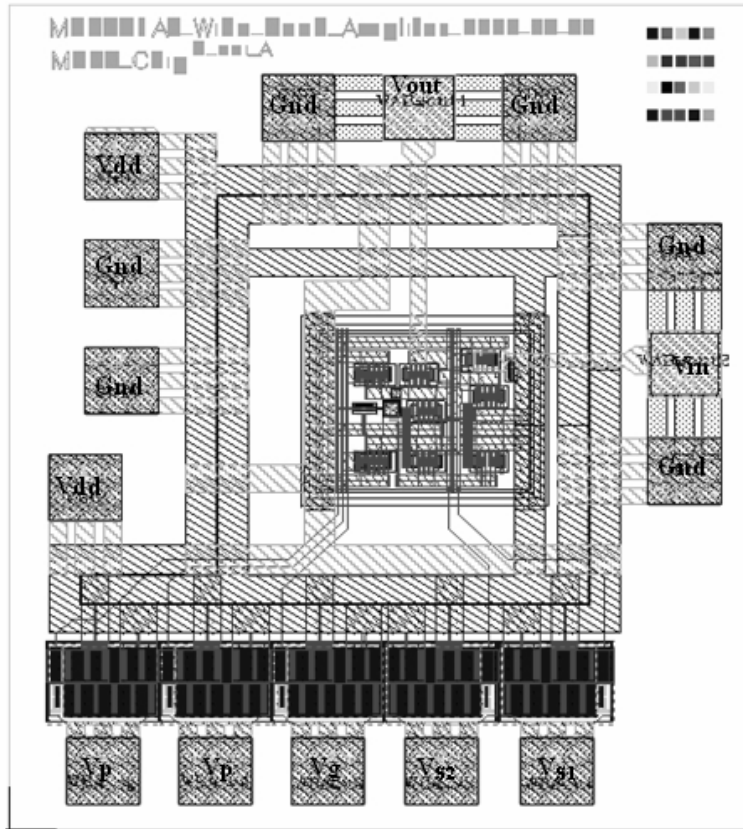
Fig. 5.16 Layout of the wide-band amplifier based on the improved active inductor

TABLE.5.2
COMPARISON OF WIDEBAND AMPLIFIERS BASED ON NOVEL ACTIVE
INDUCTOR TO OTHER DESIGNS

Wideband amplifiers	A. Worapishet [50]	W. Sansen [54]	C. K. Wang [53]	Y. C. Chen [49]	This Work
Gain (dB)	21	39	14	10.5	21
Power consumption (mW)	132	240	30	25	18
Bandwidth (GHz)	5	0.8	0.185	1.7	1
Processing (um)	0.35	1.2	0.8	0.25	0.25

5.1.5 Measurements Results

The proposed wideband amplifier is fabricated by using TSMC 0.25um CMOS process.

The photo-die and the bonding on the PCB of the wideband amplifier based on the improved

active inductor circuit are displayed in Fig. 5.17 and Fig. 5.18. In CIC, a network analyzer, a

probe station, and a Tek P6217 probe carried out the measured S-parameters and the noise figure, which demonstrate the same trend as the simulated results. According to the measures results, the performance of the wide-band amplifier can be easily observed from the S-parameters. Figs. 5.19 to 5.25 show the S-parameters and the linearlity, which compares the simulated and the measured. The bandwidth of the wideband amplifier using the improved active inductor load, which uses the RC feedback compensated network, can be expanded to a wider bandwidth than that of the wideband amplifier using the conventional cascade active inductor load. Fig. 5.24 and 5.25 indicate the results of the linearity of the wideband amplifier. The 1 dB compression and the IIP3 are about -18dBm and -14dBm, respectively. The supplied voltage VDD of this wideband amplifier is 2.5 V with 9.4-mA dc current, and the total power consumption is 23.5 mW. The maximum power gain is about 19 dB at the 1.3GHz bandwidth. Due to the additional parasitic effects in realistic fabrication, the measured results of the characteristics are smaller than the simulation results. The comparisons between the measured results and the simulated results of the wideband amplifier based on the improved active inductor are summered in TABLE 5.3.

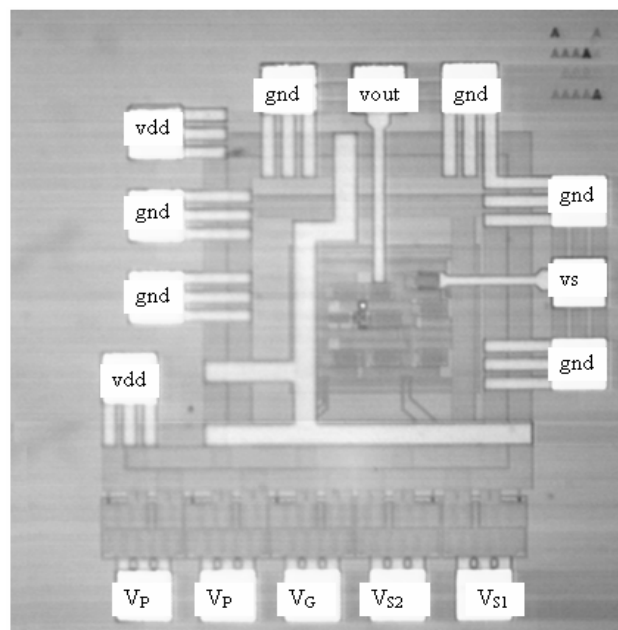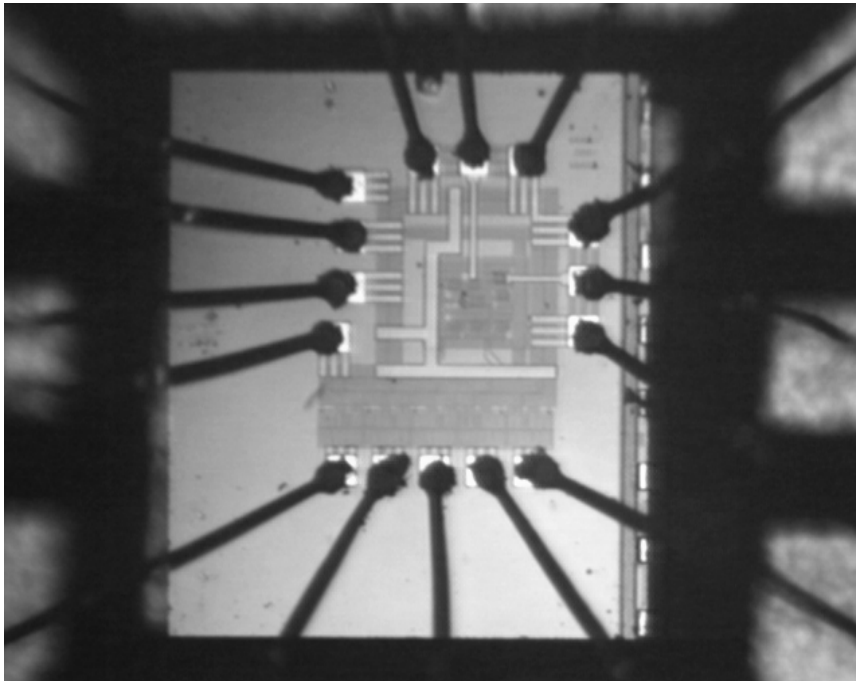Fig. 5.17 Photo-die of the wide-band amplifier

Fig. 5.18 Bonding to PCB of the proposed wide-band amplifier
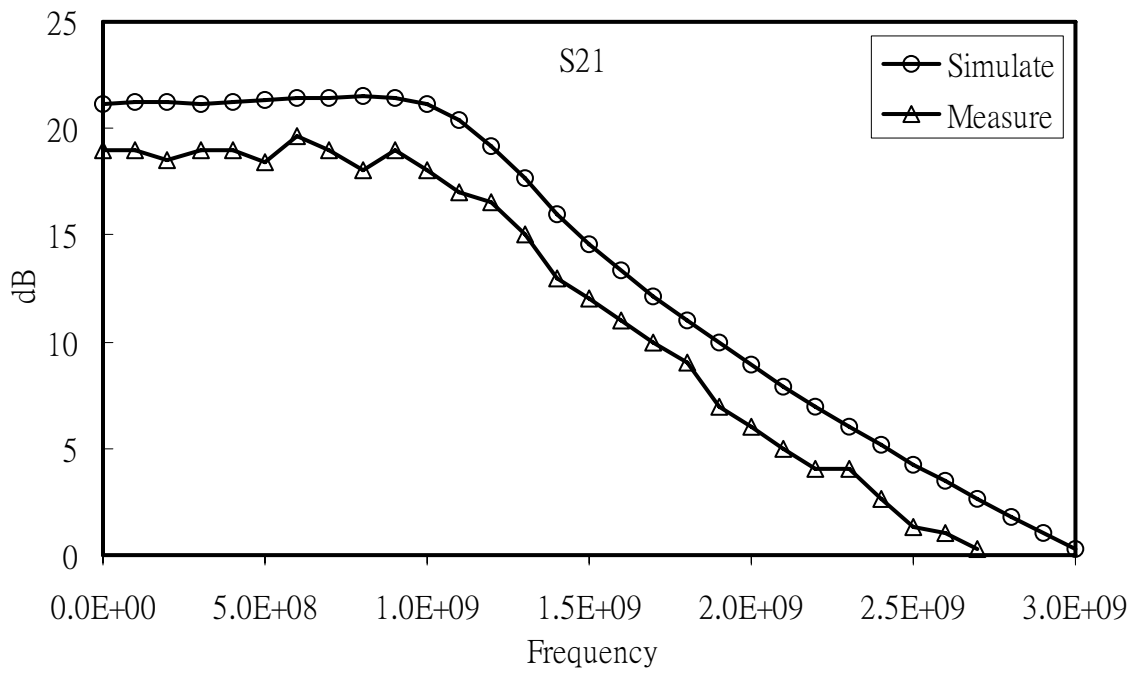
Fig. 5.19 Comprised S21 of proposed wideband amplifier
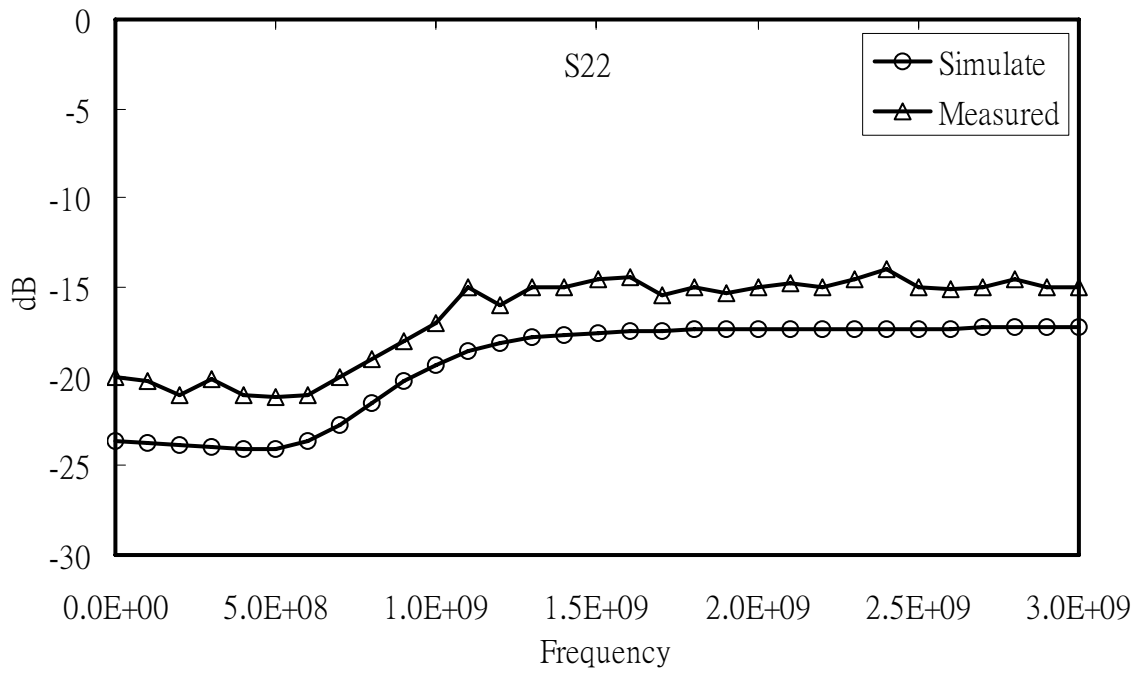
Fig. 5.20 Comprised S22 of proposed wideband amplifier
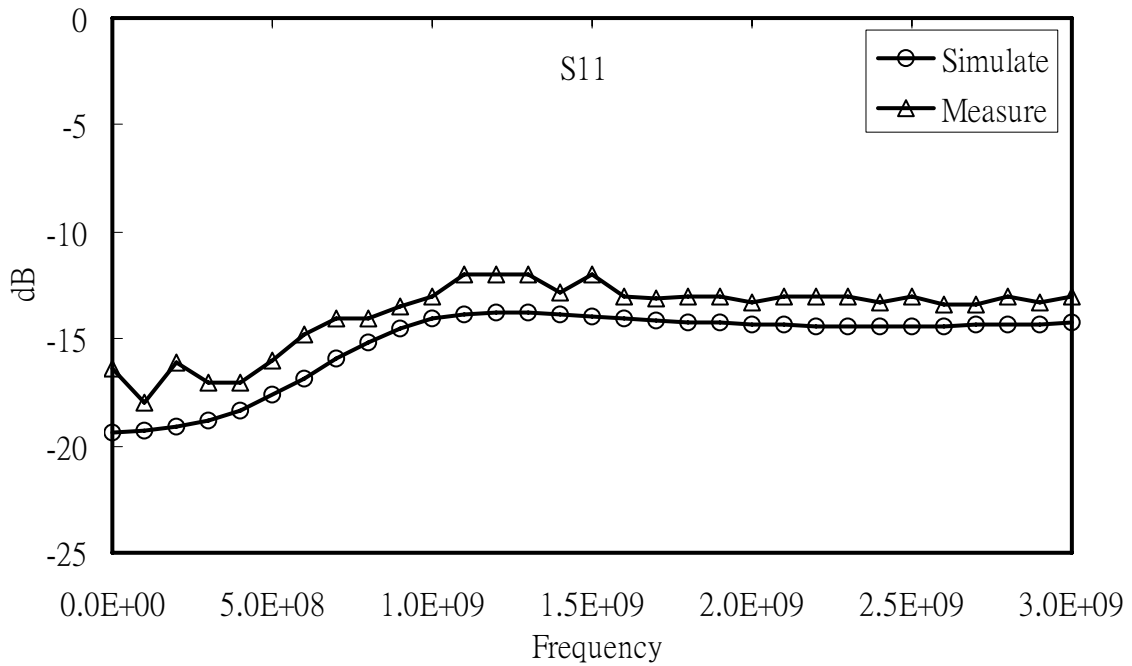
Fig. 5.21 Comprised S11 of proposed wideband amplifier
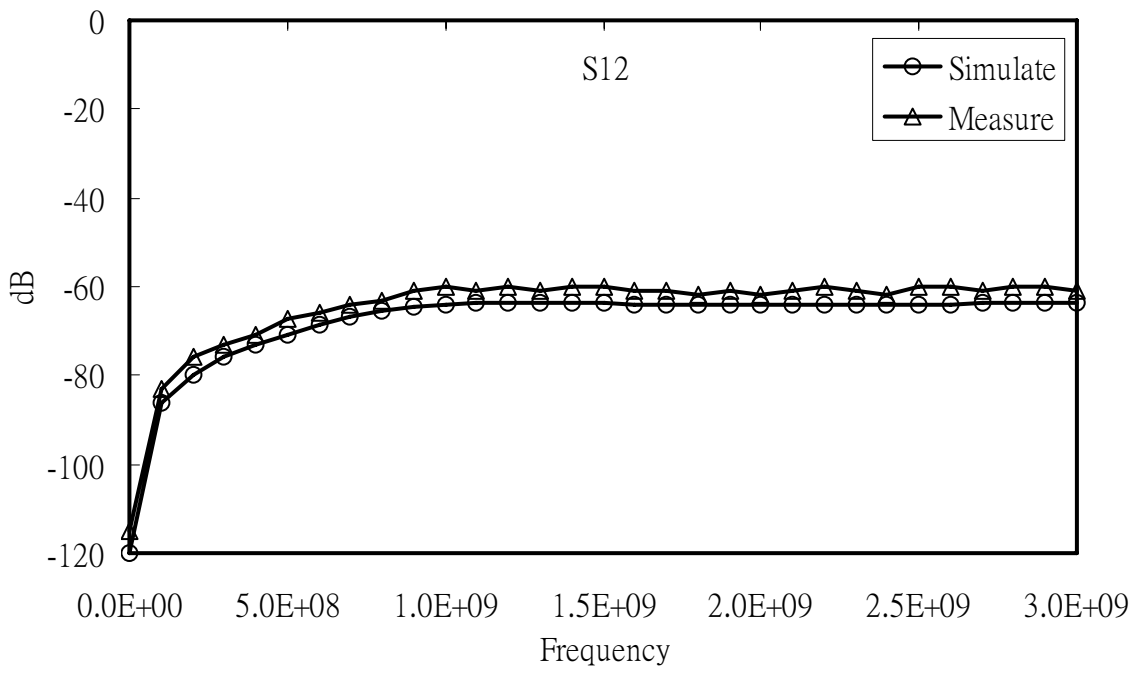
Fig. 5.22 Comprised S12 of proposed wideband amplifier
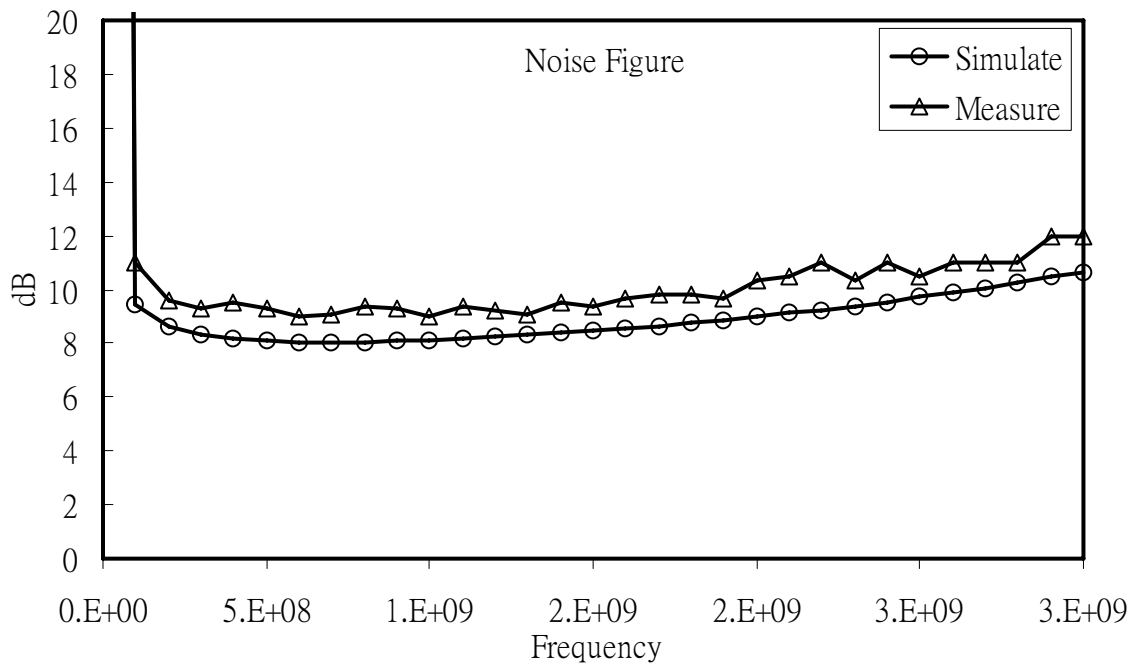
Fig. 5.23 Comprised noise figure of proposed wideband amplifier

In RF amplifier, the conditions (necessary and sufficient) for unconditional stability are expressed in following:

$$k = \frac{1 - |S_{11}|^2 - |S_{22}|^2 + |D|^2}{2|S_{12}||S_{21}|} > 1, \text{ where } D = S_{11}S_{22} - S_{12}S_{21}$$

$$|S_{12}S_{21}| < 1 - |S_{11}|^2$$

$$|S_{12}S_{21}| < 1 - |S_{22}|^2$$

From Fig. 3.5 and 3.6, at f = 1GHz, we find that K = 1.231 and D = 0.154 $\angle$ 120 $^\circ$. Since K > 1 and |D| <1, the amplifier is unconditional stable. Furthermore, in the frequency range between 0.1GHz and 1GHz shows the K > 1 and |D| <1, the amplifier will be unconditional stable.
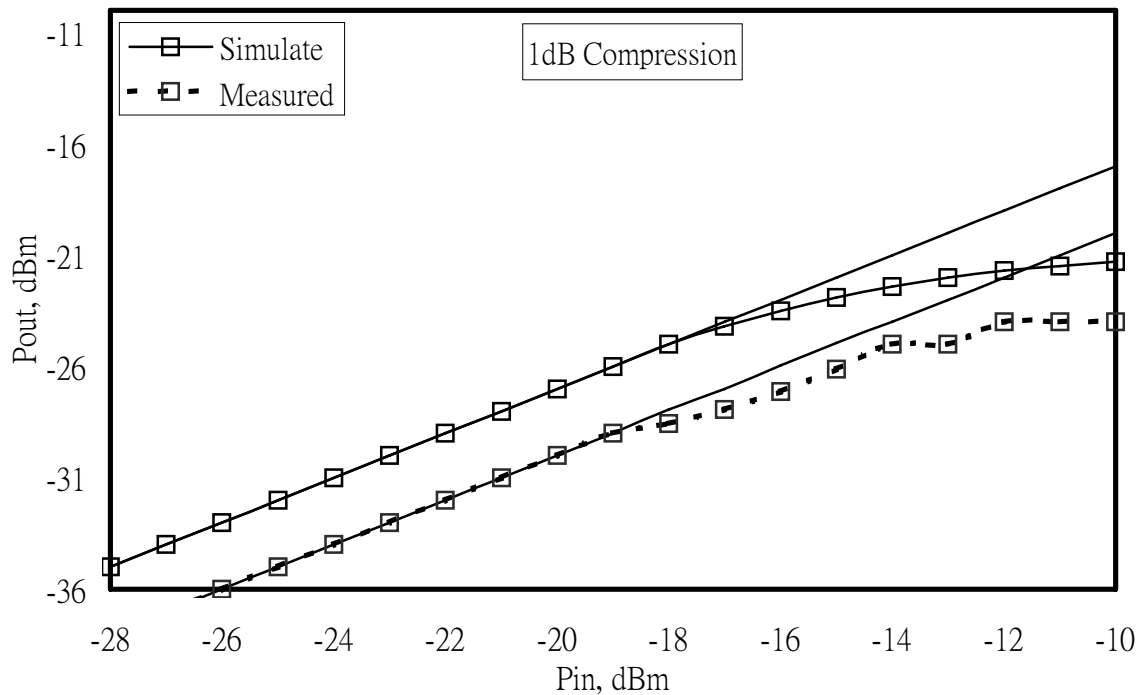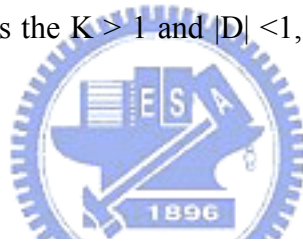
Fig. 5.24 Comprised 1dB compression of proposed wideband amplifier
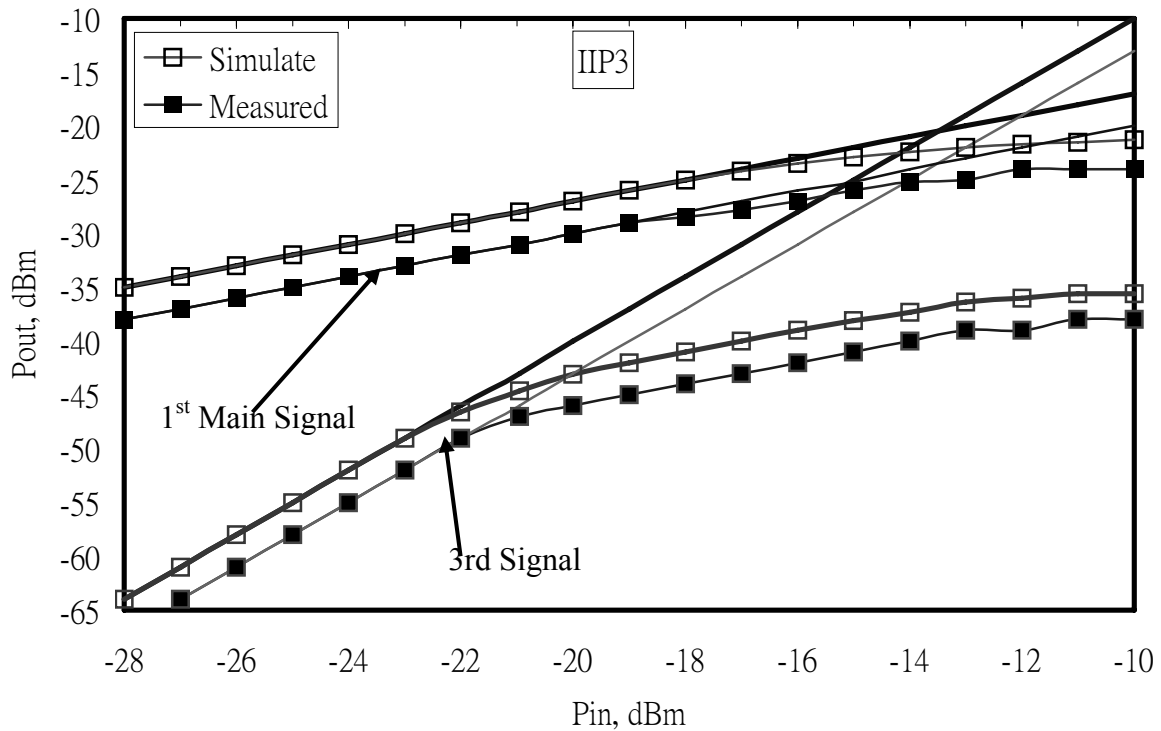
Fig. 5.25 Comprised IIP3 of proposed wideband amplifier

5.1.6 Discussion

Previous works on wideband amplifier have relied on the use of integrated passive inductors and resistors as the tuned load elements and the matching network elements. In this work, we present a CMOS wideband amplifier based on a conventional cascode active inductor load and an improved high-Q active inductor load. The proposed wideband amplifier circuit was verified by Agilent-ADS simulator, and the simulation results demonstrate that the performances of the wideband amplifier, including the bandwidth, the power gain, the noise figure and the matching features, are better than that of the previous works on CMOS broadband amplifier. Therefore, an active inductor is another attractive alternative to design a wideband amplifiers and a RF circuit. The results of this work can be applied in WCDMA mobile communication systems, optical communication systems, and WLAN transceiver systems.

TABLE 5.3 COMPARISONS BETWEEN SIMULATION AND MEASUREMENT
@ 1.3GHZ BANDWIDTH

	Simulation	Measurement
S21 (dB)	21	19
S11 (dB)	-17	-14
S22 (dB)	-21	-17
S12 (dB)	-65	-62
NF (dB)	8	9.6
Power Consumption (mW)	18	23.5
Area (mm^2)	0.713	0.713

5.2 LC Oscillator Based on Improved Active Inductor Using a Resistor

The quarter-micron or below complementary metal-oxide-semiconductor (CMOS) technology has found to be an attractive alternative to GaAs and BiCMOS technologies for the implementation of integrated radio frequency (RF) transceivers because of the lower cost concern and the possibility for integration of RF front-end and digital circuits on the same chip. Among the CMOS RF front-end blocks, an oscillator circuit is the major challenge for implementing a fully integrated transceiver because the large process parameter variations and the high Q-value passive inductors cannot easily manufactured in CMOS technology. To achieve a high-performance oscillator, the power consumption, wide tuning-range, and the stringent phase noise, need to meet the requirements in the RF circuit applications and should be simultaneously considered [12]. However, the variations of the process parameters and the low Q-value of the passive inductor fabricated in CMOS process will seriously affect these requirements. Recently, wide tuning-range ring oscillators in digital circuit and low phase noise LC oscillators using passive inductors have been demonstrated [37, 53]. On the other hand, CMOS active inductors have found in microwave/RF oscillator and these designs are

for achieving wide tuning-range and minimizing the size of the chip [54, 55]. Furthermore, three types of oscillators have been discussed. First, the LC-tuned oscillator circuits can achieve lower-phase noise, but the low Q value passive inductor limits the frequency tuning-range. Second, the ring oscillator circuits can achieve wide tuning-range, and the larger phase noise exits in ring oscillator circuit [56]. Finally, though the oscillators using active inductors have wide tuning-range, the power consumption will be sensitive affected by the frequency tuning. Therefore, it is desired to obtain an oscillator circuit based high-Q inductors so that these requirements of the constant power consumption, wide tuning-range, reasonable phase noise and phase noise deviation in spite of the variation of the frequency will be successfully achieved.

In this work, we first propose a CMOS wide tuning-range LC oscillator using improved high-Q active inductors to approach the previous requirements. The results are carried out in Agilent-ADS simulator and simulated by TSMC 0.25um CMOS process. This oscillator circuit is also biased at 2.5V as well as all transistors with the same dimension. Consequently, these results indicate that the improved inductor gets enough large Q-value. The inductor is employed in LC-tank oscillator then the wide tuning-range, which includes the range of the industry science medicine (ISM) application, can be obtained. Moreover, the power consumption will not be influenced when the frequency is varied in the wide tuned-range, and even though active inductors have higher noise than that of the passive counterparts; it still has the reasonable phase noise and phase-noise deviation.

The organization of this section is as the following. The improved high-Q active inductor design is expressed in section 5.2.1. The design of the LC oscillator circuit design based on the improved high-Q active inductor circuit is described in section 5.2.2. The simulation results of the LC oscillator circuit based on the improved high-Q active inductor are depicted in section 5.2.3. Finally, the discussion is given in section 5.2.4

5.2.1 Improved High-Q Active Inductor Design

The simplest active inductor and the small-signal equivalent circuit based on a gyrator topology are shown in Fig. 5.25 [34]. At high frequency, the circuit is equivalent to a lossy resonator. The equivalent input impedance can be expressed as (5.9) and assume $C_{gsi} >> C_{gdi}$ to obtain the following component values:

$$Z_{in} \approx \frac{(g_{ds2} + g_{m1}) + S(C_{gs2} + C_{gd1} + C_{gd2})}{(SC_{gd2} + g_{ds2} + g_{m1})(S(C_{gs2} + C_{gd1}) + g_{m2})}$$

$$G \approx g_{ds2} + g_{m1} \approx g_{m1}$$

$$L \approx \frac{C_{gs2}}{g_{m1}g_{m2}}$$

(5.9)

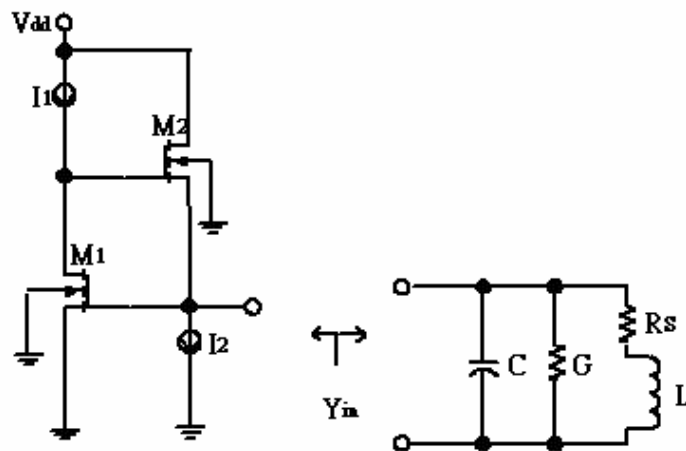$$R_S \approx \frac{g_{ds1}}{g_{m1}g_{m2}}$$

$$C \approx C_{gs1}$$

Fig. 5.26 A simple active inductor and equivalent circuit

where, the g_{mi}, g_{dsi} and C_{gsi} are the transconductance, output conductance and gate-source capacitance of correspondence transistors, respectively. The drain to the source nonideal conductance of the active devices M_P and M_S causes the internal loss increasing of active inductor. The performance of the active inductor will be disrupted such as the Q-value, operating frequency, and inductance. From Eq. (5.9), the increasing parallel conductance loss of G will reduce the Q-value of the active inductor. Therefore, in order to improve the performance such as the Q-value and the inductance (L), we propose the high-Q active inductors with a feedback resistor shown in Fig. 5.27.

The improved high-Q active inductor circuit is illustrated in Fig. 5.27 (a). It is composed of common source transistor M_1, common drain transistor M_2, feedback resistor R_f and two biasing current source I_1 and I_2. Feedback resistor R_f and transistor M_1 construct a DC gain network. This network produces a gain factor to reduce the parallel conductance (G). Furthermore, the internal loss of the inductor can be decreased and the Q value can also be increased. Thereby, the inductance (L) is also increased due to the feedback resistor. At high frequency, this circuit is equivalent to a lossy resonator as well, which is shown in Fig. 5.27 (b). The values of each component including three parameters, C_{gs}, g_{ds}, and g_m for analyzing this circuit are demonstrated below.

$$G \approx g_{ds2} + \frac{g_{m1}}{1+R_f g_{ds1}}$$

$$L \approx \frac{C_{gs2}\left(1+R_f g_{ds1}\right)}{g_{m1} g_{m2}} \tag{5.10}$$

$$R_s \approx \frac{g_{ds1}}{g_{m1} g_{m2}}$$

$$C \approx C_{gs1}$$
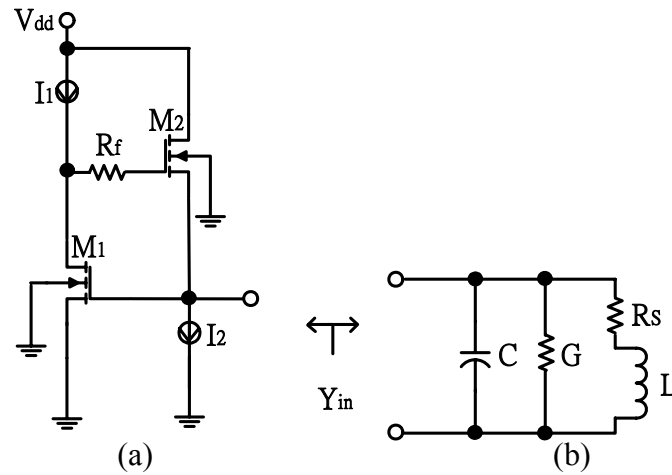
Fig. 5.27 Proposed high-Q active inductor and equivalent circuit

From Eq. (5.10), the effect of the factor, $(1+ g_{ds1}R_f)$, is designed to be a value greater than unity. The equivalent parallel conductance loss (G) changes from $g_{ds2} + g_{m1}$ to $g_{ds2} + \dfrac{g_{m1}}{1+ g_{ds1}R_f}$, and then the loss is minimized by a $(1+ g_{ds1}R_f)$ factor. In Eq. (10), the equivalent inductance changes from $\dfrac{C_{gs2}}{g_{m1}g_{m2}}$ to $\dfrac{C_{gs2}(1+ g_{ds1}R_f)}{g_{m1}g_{m2}}$, and then the inductance is also increased by a $(1+ g_{ds1}R_f)$ factor. Therefore, the Q-value and the inductance (L) of the inductor are greatly increased. As a result, the performance of the inductor can be significantly improved by using a simple loss compensation of a feedback resistor (R_f). Furthermore, the circuit of the active inductor is simpler than that of the other circuits published previously. If the circuit components are properly chosen, a higher Q-value and a higher inductance value can be realized.

All simulations are carried out in an Aligent-ADS simulator. The active devices are modeled by TSMC 0.25um CMOS process at 2.5V. All transistors have the same dimensions, where the length and width of each MOSFET are 0.24 um and 40 um, respectively. The result of scattering parameter (S11) performance of the inductor is exposed in Fig. 5.28. This figure

can be treated as, the curve follows the increasing of the feedback resistance R_f between 0.8GHz and 3GHz, the moving trend of this curve inclines to the outside of the circle, indicating that the loss is decreased, but the Q-value is increased. Therefore, the Q-value is promoted with the feedback resistance, shown in Fig. 5.29. Here, the Q-value is increased follow-up the increasing feedback resistor value. In Fig. 5.30, according to Eq. (10), the inductance (L) of inductor is also increased by the increasing feedback resistance R_f in the range of 0.8GHz to 3GHz. As a result, the performance of the inductor including the Q value and inductance may be improved with a simple loss compensation network. In addition, the current does not pass the feedback resistance, and the power consumption of the inductor will not be changed when the feedback resistance varies the characteristics of the inductor. Thus, the unchanged power consumption characteristic can be applied to design a constant power consumption wide tuning-range oscillator circuit.
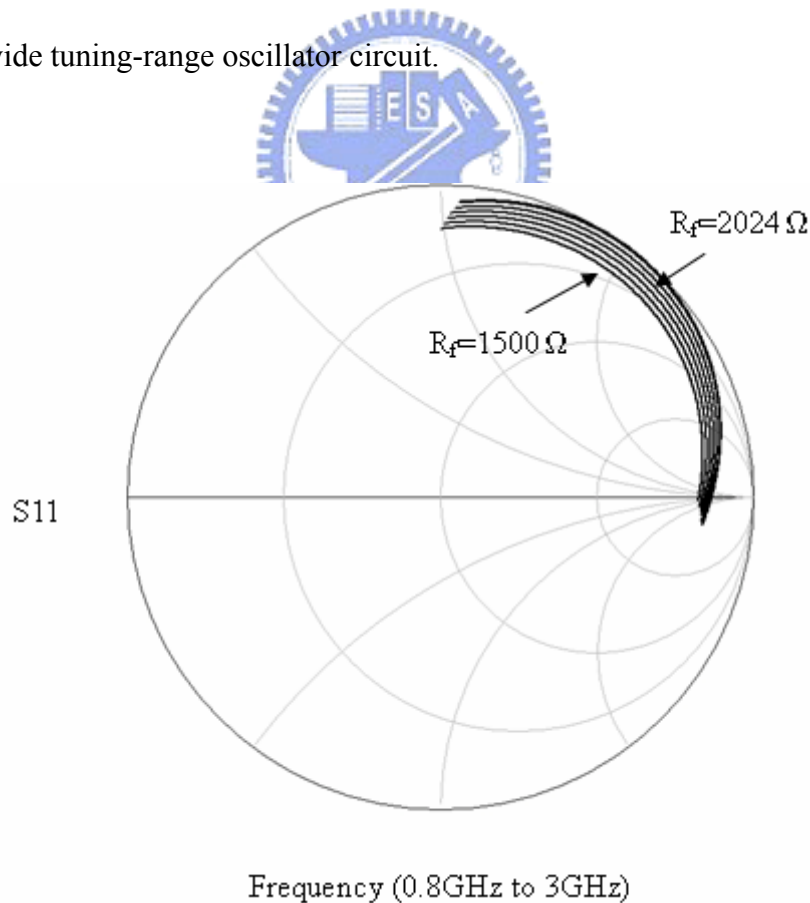
Fig. 5.28 S11 performance of high-Q active inductor

The improved active inductor only uses a feedback resistor to obtain the characteristics of the high-Q and the constant power consumption. Based on the improved high-Q active inductor, the LC oscillator can be easily designed. The LC oscillator can achieve the required performances such as the wide-tuning frequency, the reasonable phase noise, and the constant power consumption.
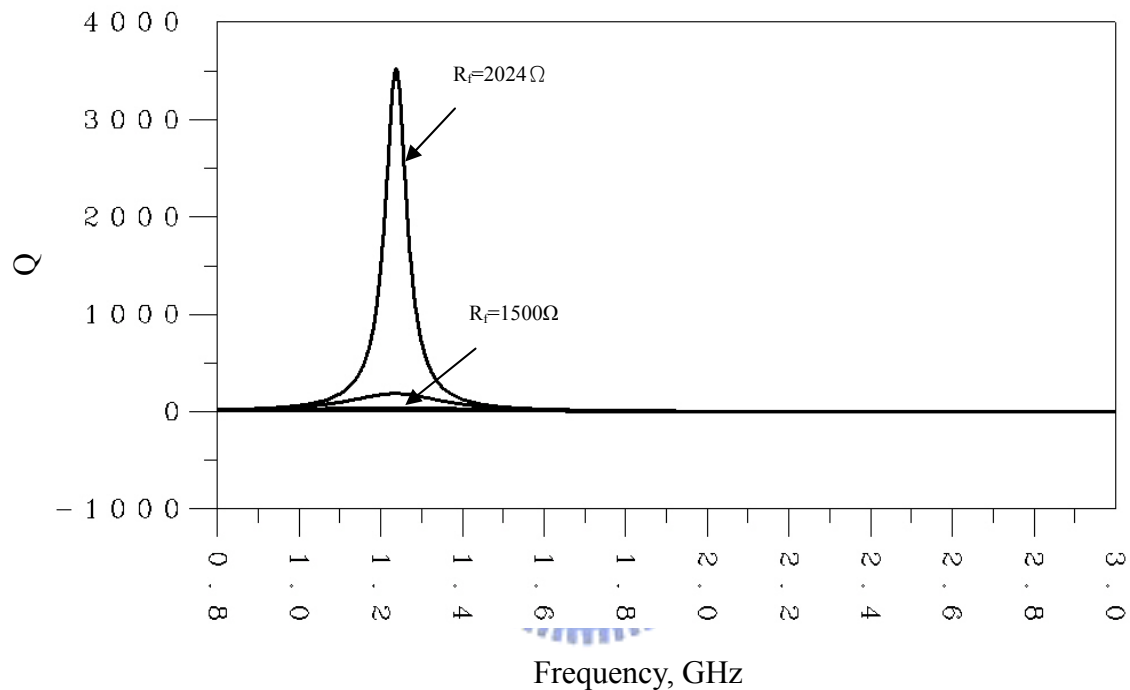
Fig. 5.29 Q value of High-Q active inductor

5.2.2 Oscillator Circuit Design

The main design consideration of the oscillator is expected to obtain low constant power consumption, wide tuning-range and low phase noise. The circuit diagram of the proposed LC oscillator is shown in Fig. 5.31. This design has a cross-coupled connection of NMOS transistors M_{NR} and M_{NL}. The cross-coupled connection generates a positive feedback loop for providing negative resistance, called a negative impedance converter (NIC). The

NIC configuration compensates the loss of the active inductor in the LC tank to produce lossless LC tank. The inductor of the LC tank is used to improve high-Q active inductors and is shown in Fig. 5.27 (a). The active inductors are composed of M_{1R}, M_{1L}, M_{2R}, M_{2L}, M_{SR}, M_{SL}, M_{PR}, M_{PL}, R_{fR} and R_{fL}, which combine with the NIC to form the LC resonators. Two active inductors are acting as the equivalent inductance in the oscillator. Because this oscillator circuit is symmetric and the Q value of the active inductor is high enough, all transistors have the same minimum dimension, where the length and width of each MOSFET are 0.24um and 40um, respectively. No varactors are employed in this oscillator. The oscillator frequency modulation function can be achieved by using the resistors of the active inductor.
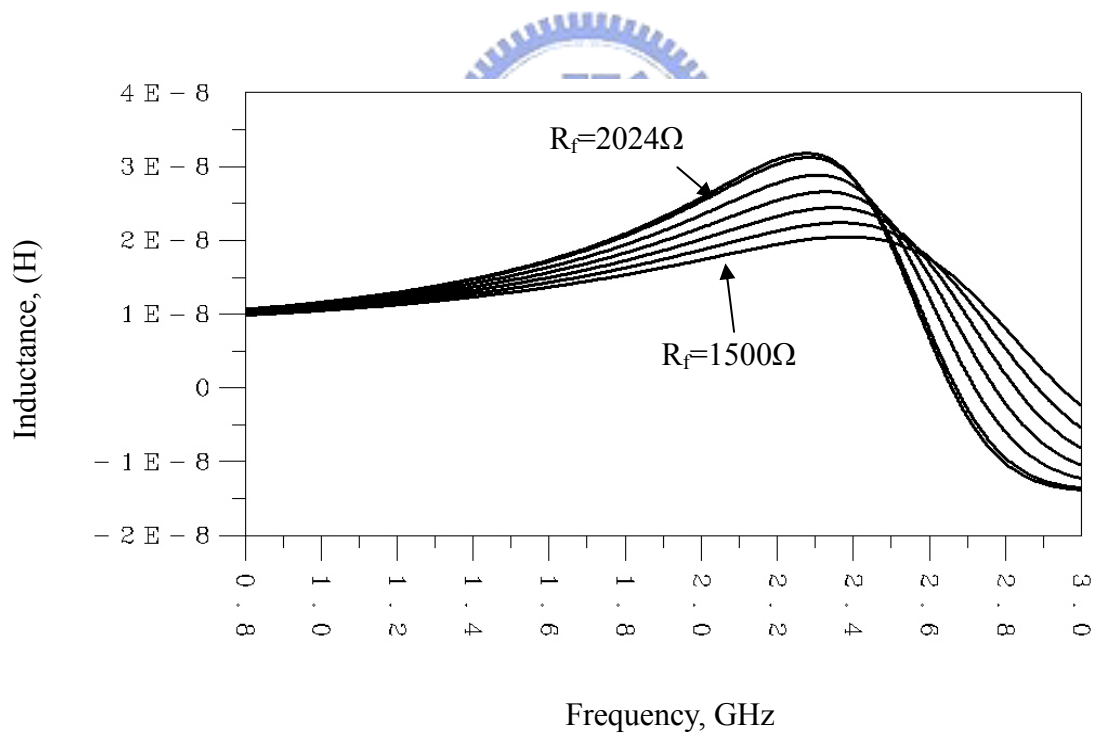
Fig. 5.30 Inductance of High-Q active inductor

To provide adjustable frequency range, the feedback resistance R_f is added to tune the desired oscillator frequency. Because the equivalent inductance values are varied by the

resistance R_f, the capacitance is kept unchanged. Besides, the frequency of the oscillator can tune the bias of the active inductors. Thus, the resistors Rf and the bias of the active inductor can adjust the output frequency of the oscillator.

Assuming the total equivalent capacitance from the output node of the NIC is C_T, the output oscillating frequency can be expended as:

$$\omega_0 \approx \sqrt{\frac{g_{m1}g_{m2}}{(C_{gs1}+C_T)[C_{gs2}(1+R_f g_{ds1})]}} \qquad (5.11)$$

Fig. 5.31 Proposed LC Oscillator

5.2.3 Simulation Results

From Eq. (5.11), the frequency ω_o is the inverse proportion of the feedback resistance R_f. In other words, when the feedback resistance is decreased, the frequency will be increased, and vice versa. The output frequency shows a wide tuning frequency range. The result between the output frequency and the feedback resistance is given in Fig. 5.32. This figure points out the frequency with the feature of a wide tuning-range, from 0.8GHz to 3GHz. Although the wide tuning frequency range is achieved, the power consumption is still constant. Fig. 5.33 shows the constant power consumption of 10mW. The power consumption is constantly maintained in the range of 0.8GHz and 3GHz. The relationship between the output amplitude and the output frequency is appeared in Fig. 5.34. It indicates that the variation of the output amplitude is about 15dBm at the wide tuning-range of 0.8GHz to 3GHz. At the 1MHz offset, the phase noise in the wide tuning-range is exposed in Fig. 5.35. It explores that the variation of the phase noise at the range of 0.8GHz and 3GHz is about 6dBc/Hz and the phase noise almost retains a constant value between 1.5GHz and 3GHz. Moreover, the oscillator has the reasonable phase noise below -91dBc even though the active inductors have the higher noise than the passive counterparts. Finally, this proposed circuit exhibits the wider tuning-range, constant power consumption, and the reasonable phase-noise. The layout of the proposed LC voltage-controlled oscillator is shown in Fig. 5.36. The size of the proposed circuit is about 1065um $\times$ 482um. The size of the oscillator is smaller than that of the voltage-controlled oscillator using passive spiral inductor. The comparison between the CMOS wideband amplifier based on the improved active load and the other published works [35, 37] is also shown in TABLE 5.4. From the comparison, our work is superior to those wideband amplifiers in some features.

5.2.4 Discussion

A CMOS LC oscillator using an improved high Q-value active inductor is proposed. By using a feedback resistor R_f, the active inductor can achieve high Q-value and the inductance (L) can be tuned as well but the power consumption is still constant. The power consumption of the oscillator based on the active inductors can be retained a constant value in a wide frequency tuning range. The phase noise has the reasonable value even though the active inductor has larger noise than the passive inductor counterparts. These simulation results of the proposed circuit are better than that of the previously literatures [54-56]. Therefore, this study shows that the proposed circuit with simulation can achieve a constant power consumption, wide frequency tuning-range and reasonable phase noise.
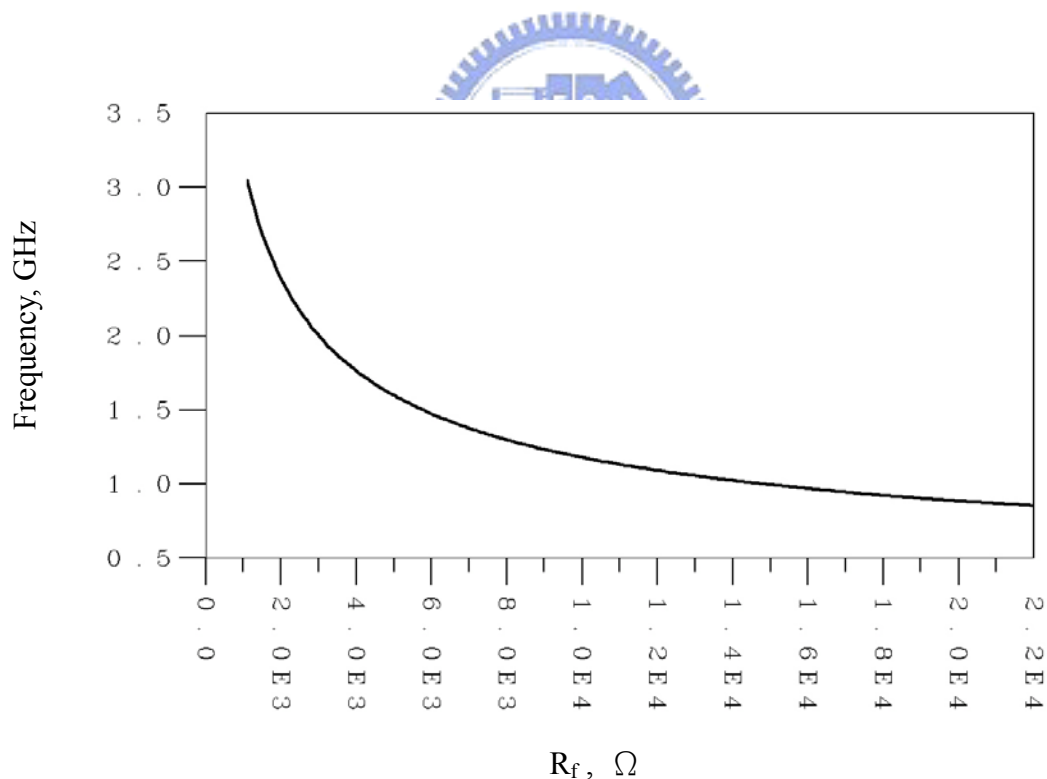
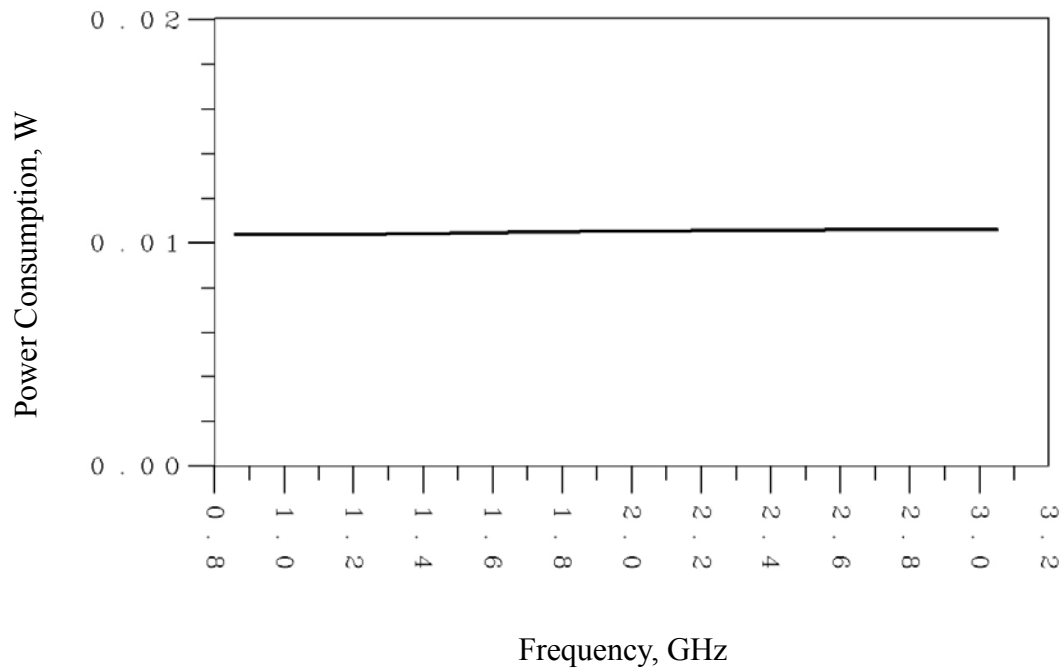Fig. 5.32 Frequency of output V.S. feedback resistance R_f

Fig. 5.33 Oscillator power consumption V.S. tuning frequency
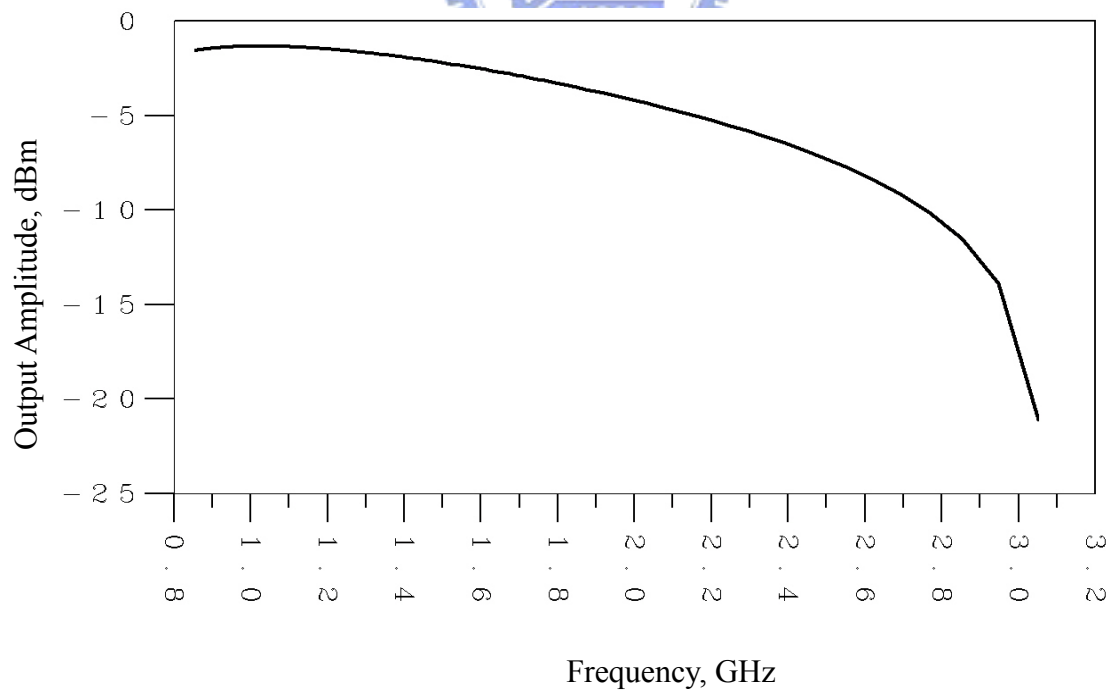
Fig. 5.34 Output amplitude V.S. tuning frequency
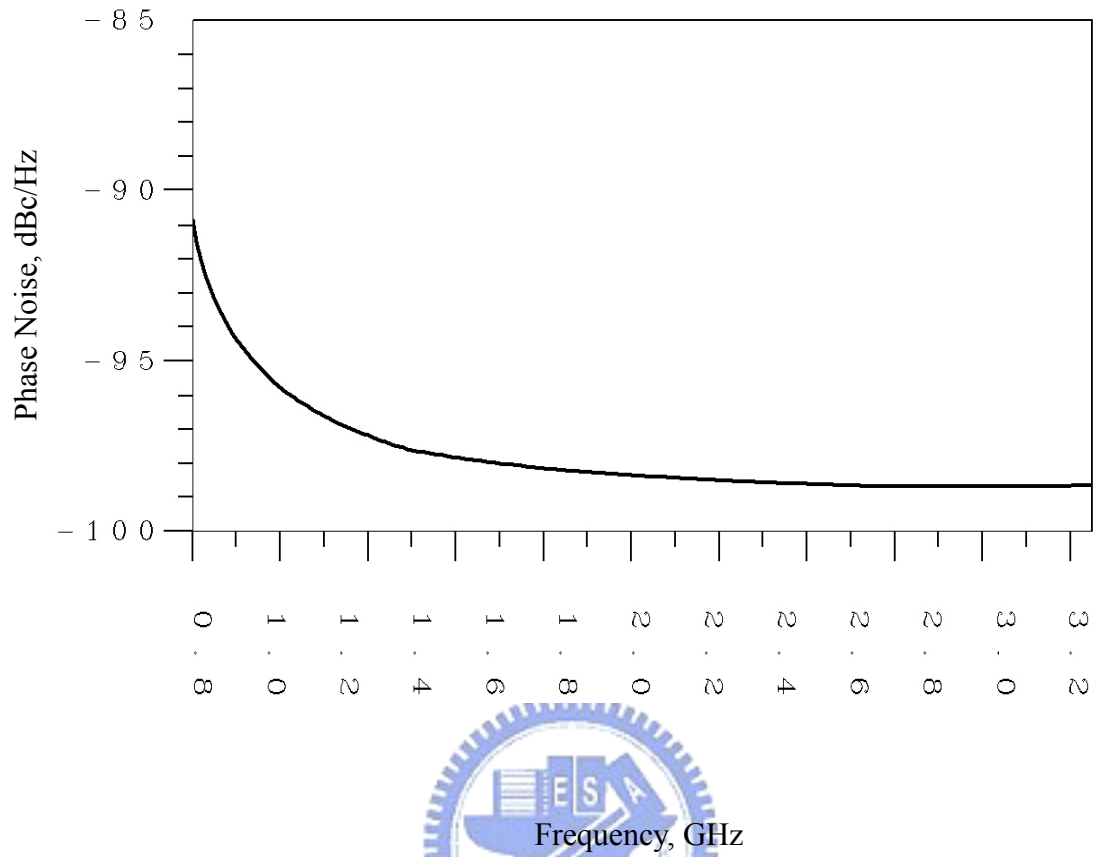
Fig. 5.35 Phase noise V.S. tuning frequency
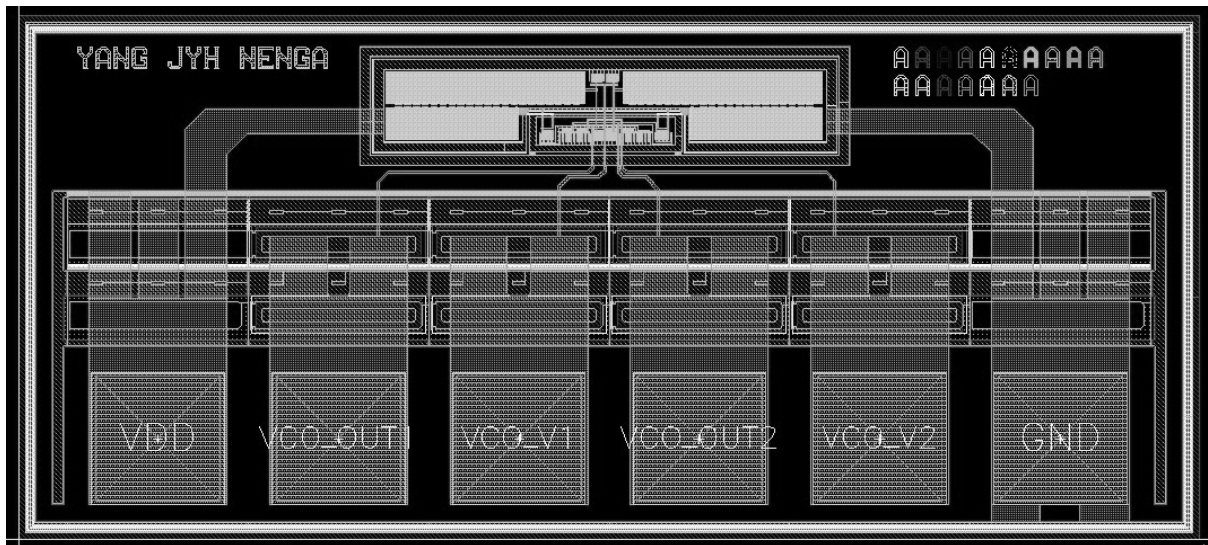
Fig. 5.36 Layout of the proposed VCO

TABLE 5.4 COMPARISON OF VCO WITH OTHER WORKS

	T.K. Lin (35)	Y. Wu (37)	This work
Frequency (GHz)	1.5	0.9	1.5
Tuning Range (GHz)	1.1 - 2.1	0.1 - 0.9	1 - 3
Phase Noise (dBc/Hz)	-83	-86	-98
Power Consumption (mW)	50	46	10
Inductor	Active	Active	Active

5.3 Summary

In this chapter, the wide-band amplifier and the voltage-controlled oscillator based on the improved active inductor are presented. The improved active inductors can achieve the high gain-bandwidth of the wide-band amplifier and the reasonable performance of the voltage controlled oscillator. Furthermore, the chip size can be reduced as well. Thus the improved active inductor based on a cascode RC feedback loss compensated technique is very suitable to be used in wide-band amplifier. The improved active inductor only uses a resistor to compensate the loss of the active inductor and it can be applied in voltage-controlled oscillator. The VCO can achieve the const power consumption, the wide tuning range, and the reasonable phase noise. Besides, the variation of the phase noise can also remain small in wide frequency range.

Chapter 6

Conclusions and Future Works

In this dissertation, we have proposed the radio frequency (RF) CMOS low noise amplifier circuits using active inductors so that these circuits can operate in different frequency band. This design can achieve high performance and save the chip size in IC fabrication. For active inductor circuits, we also proposed loss compensated techniques to improve the characteristics of the active inductors such as the quality factor, the inductance, and the operating frequency. This design simplifies the circuit configuration of the active inductors. Furthermore, the wide-band amplifier circuit and the voltage controlled oscillator circuit based on the improved active inductors are proposed as well. As a result, these proposed circuits could achieve the requirements of designing and minimizing the chip size.

An interaction of active devices can use a gyrator configuration to simulate the characteristic of the inductance impedance, which is called active inductor. The inductance impedance is combined by a real term and an imagine term. The real term is also called the loss of the inductance impedance. According to the real term and the imagine term, quality factor, inductance, loss, and resonant frequency can be defined. These definitions can be used to explore the characteristics of the active inductor and to improve the active inductor. By using the inductance impedance, an active inductance can be applied in a RF circuit to act as a load and to obtain impedance matching.

The proposed 2.06GHz/2GHz RF CMOS low noise amplifiers utilize regulated cascode active inductor load and common source negative conductance generator to complete the amplifier design. The combination of the regulated cascode active inductor and source follower negative conductance generator are mainly increased the quality factor to obtain the high impedance load. As a result, the amplifiers achieve high power gain and good input/output impedance matching. And the size of the amplifier is less than that of the amplifier using the passive spiral inductor due to only using active inductor. In addition, by changing the external bias voltage, the amplifiers are able to operate in different frequency bands.

The proposed 1.75GHz/2.4GHz RF CMOS low noise amplifiers use the cascode active and double feedback loss compensated technique to realize the amplifier design. The double feedback loss compensated circuit can reduce the loss of the cascode active inductor and raise the load impedance. Therefore, the amplifiers gain the characteristics of high power gain, and good input/output matching. By way of the external bias voltage the amplifiers can operate in various frequency bands. Furthermore, the chip size is reduced because of employing without any passive spiral inductor

Nevertheless, the techniques of using common gate/source follower negative conductance generator are to increase the load impedance. The amplifiers will result in complexity circuit. Thus, the simple loss compensated approaches are proposed to improve the characteristics of the active inductor and further apply in RF amplifier for obtaining better results.

The proposed high-Q active inductor utilizes a RC feedback loss compensated technique to improve the Q-value, inductance, and the operating frequency. The improved active inductor based on a simple RC feedback network produces the negative conductance to compensate the loss due to the nonlinear active devices. The proposed high-Q active inductor

is designed based on the techniques of the current-reused and gain-boosting. The feedback can improve the performances of the active inductor such as the Q-value, the inductance, and the operating frequency. The proposed high-Q active inductor using a capacitor is able to compensate the loss of the active devices. A simple high-Q active inductor circuit can easily obtain. The proposed high-Q active inductor employs the technique of only using a resistor to compensate the loss of the active device. The performances of the active inductor such as the Q-value, the inductance, and the operating frequency can be significantly improved. And the circuit is very simple.

The proposed wide-band amplifier employs the improved active inductor, which uses the loss compensated technique of the RC feedback circuit. The wide-band amplifier can achieve wide frequency bandwidth, high enough power gain, and reasonable noise figure. And the size of the wide-band amplifier is smaller than that of the wide-band amplifier using the passive spiral inductor or the resistor. The proposed voltage controlled oscillator exploits the improved active inductor, which bases on the loss compensated technique of a resistor. The voltage-controlled oscillator has constant power consumption and reasonable phase noise.

In the pervious works and the literatures, comparing with the designs using a passive spiral inductor, the active inductors have many advantages such as the higher Q-value, the higher inductance, the electrical tunable, and the smaller chip size. Although, the design of the active inductors is reaching our current goals, there are still some shortcomings existing in active inductor such as the power consumption, the noise, and the dynamic range. Because the active inductors are comprised of the active devices, the active inductor will produce noise, power consumption, and the limitation of the dynamic range. Therefore, reducing the noise, decreasing the power consumption, and increasing the dynamic range are our main objects in the future works. If these problems can be solved, the active inductors applying in

RF CMOS circuit could be an alternate approach. Finally, the active inductors have many merits to apply in RF circuit designs.

References:

[1] A. D. Kucar, "Mobile Radio: An Overview," *IEEE Commun. Mag.,* pp. 72-85, Nov. 1991.

[2] R. Fujimoto, and K. Kojima, "A 7-GHz 1.8-dB NF CMOS Low-Noise Amplifier," *IEEE International Solid-State Circuits*, Vol. 37, pp. 852-856, July 2002.

[3] A. Ismail and A. Abidi, "A 3 to 10GHz LNA Using a Wideband LC Ladder Matching Network," *ISSCC Dig., Tech. Papers*, pp. 384-385, Feb. 2004.

[4] J. Min *et al.*, "An All-CMOS Architecture for a Low-power Frequency-hopped 900 MHz Spread Spectrum Transceiver," in *Proc.CICC,* pp. 16.1.1 - 16.1.4, May 1994.

[5] A Bevilacqua et al., "An Ultra-Wideband CMOS LNA for 3.1 to 10.6GHz Wireless Receiver," *ISSCC Dig., Tech. Papers,* pp. 382-383, Feb. 2004.

[6] J. Y. C. Chang and A. A. Abidi, "A 750 MHz RF Amplifier in 2-um CMOS," in *Symp. VLSI Circuits Dig. Tech., Papers*, pp. 111-112 1992.

[7] A. N. Karanicolas, "A 2.7 V 900 MHz CMOS LNA and Mixer," in *ISSCC Dig. Teach. Papers*, pp. 50-51, Feb. 1996.

[8] D. Allstot et al., "Design Considerations for CMOS Low-Noise Amplifiers," *RFIC*, pp. 97-100, 2004.

[9] A. Rofougaran *et al.*, "A 1 GHz CMOS RF Front-end IC with Wide Dynamic Range," in *Proc. ESSCIR,* pp. 250-253, 1995.

[10] J. Carols, and M. S. J. Steyaert, "A 1.5 GHz Highly Linear CMOS Down Conversion Mixer," *IEEE Journal of Solid-State Circuits*, Vol. 30, pp. 736-742, July 1995.

[11] M. Brandolini, P. Rossi, and D. Sanzogni, "A CMOS Direct Down-Converter with +78dBm Minimum IIP2 for 3G Cell-Phones," in *ISSC Dig. Tech. Paper* pp. 320-321, Feb., 2005.

[12] L. Zhenbiao, and O. Kenneth, "A 900 MHz 1.5 V CMOS Voltage-Controlled Oscillator Using Switched Resonators with a Wide Tuning Range," *IEEE Microwave and Wireless Components Letter*, Vol. 13, No. 4, April 1997.

[13] Y. K. Chu, and H. R. Chung, "A Fully Integrated 5.8 GHz U-NII Band 0.18-um CMOS VCO," *IEEE Microwave and Wireless Components Letter*, Vol. 13, No. 7, July 1997.

[14] D. Guermandi, et al., "A 0.75 to 2.2GHz Continuously-Tunable Quadrature VCO," *ISSCC Dug. Tech. Paper,* pp. 536-537, Feb., 2005.

[15] C. Y. Wu, and S. Y. Hsiao, "The Design of a 3 V 900MHz CMOS Bandpass Amplifier, " *IEEE Journal of Solid-State Circuits*, Vol. 32, No. 2, pp. 159-168, Feb. 1999.

[16] M. Rofougaran *et al.*, "A 900Hz CMOS RF Power Amplifier with Programable output," in *Sym. VLSI Circuits Dig. Tech. Papers* pp. 133-134 1994.

[17] P. Reynaert and M. Steyaert, "A 1.75GHz GSM/EDGE Polar Modulated CMOS RF Power Amplifier," in *ISSCC Dig. Tech. Paper,* pp. 536-537, Feb., 2005.

[18] A. Rofougaran, J. Y-C Chang, M. Rofougaran, A. A. Abidi, "A 1 GHz CMOS RF Front-End IC for a Direct-Conversion Wireless Receiver," *IEEE Journal of Solid-State Circuits*, Vol. 31, pp. 880-889, July 1996.

[19] D. K. Shaffer, and T. H. Lee, "A 1.5 V, 1.5 GHz CMOS Low Noise Amplifier," *IEEE Journal of Solid-State Circuits*, Vol. 32, pp. 745-759, May 1997.

[20] A. N. Karanicolas, "A 2.7 V 900 MHz CMOS LNA and Mixer," *IEEE Journal of Solid-State Circuits*, Vol. 31, pp. 1939-1944, Dec. 1996.

[21] C. S. Kim, M. Park, C.H. Kim, H. K. Yu, and E. H. Cho, "Thick Metal CMOS Technology on High Resistivity Substrate and its Application to Monolithic L-Band CMOS LNAs," *Etri Journal*, Vol. 21, No. 4, pp. 1-8, Dec. 1999.

[22] V. Aparin, et al., "A Full-Integrated Highly Linear Zero-IF CMOS Cellular CDMA Receiver," *ISSCC Dug. Tech. Paper,* pp. 324-325, Feb., 2005.

[23] Fraunhofer Institute Angewandte (FhG/IAF): Design Kit for Monolithic Microwave Integrated Circuits (MMIC), Junuary 1997.

[24] H. M. Greenhous, "Design of Planar Rectangular Microelectronic Inductors," IEEE Trans. Parts, Hybrids and Packaging, Vol. PHP-10, pp. 101-109, June 1974.

[25] J. N. Burghartz, K. A. Jenkins, and M. Soyuer, "Multilevel-Spiral Inductors Using VLSI Interconnect Technology," *IEEE Electron Device Letters*, Vol. 17, No. 9, pp. 428-430, Sep. 1996.

[26] J. N. Yang and C. Y. Lee *et al.*, "A 1.5-V 2.4 GHz CMOS Low Noise Amplifier," *Proceedings of the 43rd IEEE Midwest Symposium on Circuit and System*, Vol. 2, pp.1010-1012, Aug. 2000.

[27] S.Hara, T. Tokumitsu, T. TanaKa. and M. Aikawa,"Broad-Band Monolithic Microwave Active Inductors and Its Application to Miniaturized Wide-Band Amplifier," *IEEE Transaction on Microwave Theory and Techniques*, Vol. 36, No. 12 pp. 1920-1924, Dec. 1988.

[28] S. Hara, T. Tokumitsu, and M. Aikawa, "Lossless Broad-Band Monolithic Microwaves Active Inductor," *IEEE Transaction on Microwave Theory and Techniques*, Vol. 37, No. 12 pp. 1979-1983, Dec. 1989.

[29] S. Lucyszyn, and I. D. Robertson, "Monolithic Narrow-Band Fiter Using Ultrahigh-Q Tunable Active Inductor," *IEEE Transaction on Microwave Theory and Techniques*, Vol. 42, No. 12 pp. 2617-2622, Dec. 1994.

[30] H. Hayashi, M. Muraguchi, Y. Umeda, and T. Enoki, "A High-Q Broad-Band Active Inductor and Its Application to a Low-Loss Analog Phase Shifter," *IEEE Transaction on Microwave Theory and Techniques*, Vol. 44, No. 12 pp. 2369-2374, Dec. 1996.

[31] A. Thanachayanont, *et al.*, "A 3 V RF CMOS Bandpass Amplifier Using an Active Inductor," in *IEEE Conference*, pp. I440-I443, March, 1998.

[32] W. Zhuo, *et al.*, "Programmable Low Noise Amplifier with Active Inductor," *IEEE Conference*, pp. IV365-IV368, March 1998.

[33] M. Ismail, R. Wassenaar, and W. Morrison, "A High-Speed Continuous-Time Bandpass VHF Filter In MOS Technology," *Proc. IEEE ISCAS*, Vol. 3, pp. 1761 -1764, April 1991.

[34] A. Thanachaynont, and A. Payne, "VHF CMOS integrated active inductor," *Electron. Lett.,* Vol. 32, No. 11, pp. 999-1000 May 1996.

[35] T.K. Lin, and A.J. Payne, "Design of a Low-Voltage, Low-Power, Wide-Tuning Integrated Oscillator," *IEEE ISCAS*, pp. V-629-V-632, June 2000.

[36] Y. Wu, X. Ding, M. Ismail, and H. Olsson, "Inductorless CMOS RF bandpass filter," *Electron.Lett.,,* Vol. 37, No. 16, pp. 1027-1028, April 2001.

[37] Y. Wu, M. Ismail, and H. Olsson, "CMOS VHF/RF CCO based on active inductors," *Electron.Lett.*, Vol. 37, No. 8, pp. 472-473, April 2001.

[38] U. Yoaprasit and J. Ngarmnil, "Q-Enhancement technique for RF CMOS active inductor," *Proc. IEEE ISCAS*, Vol. 5, pp. 592-598, 2000.

[39] Y. Wu, X. Ding, M. Ismail, and H. Olsson, "A novel CMOS fully differential inductorless RF bandpass filter," *Proc. IEEE ISCAS*, Vol. 4, pp. 149-152, 2000.

[40] R. Kaunisto, P. Alinkula, and K. Stadius, "Active Inductors for GaAs and Bipolar technologies," Analog Integrated Circuits Signal Processing, Vol. 7, No. 1, pp. 35-48 1995.

[41] Hsiao C. C., Kuo C. W., C. C. Ho, and Chan Y. J.: 'Improved Quality-Factor of 0.18-um CMOS Active Inductor by a Feedback Resistance Design', *IEEE Microwave and Wireless Components Letters*, Vol. 12, pp. 467-469, 2002.

[42] Chen-Yi Lee, Jyh-Neng Yang, and Yi-Chang Cheng, "Improving RF CMOS Active Inductor by Simple Loss Compensation Network," *IEICE Transaction Communication*,

Vol. E87-B, No. 6, pp. 2195-2198, June 2004.

[43] G. D. Vendelin, A. M. Pavio, and U. L. Rohde, "Microwave circuit design using linear and nonlinear techniques," (*John Wily & Sons, New York*, 1990)

[44] T. T. Y. Wong, "Fundamentals of Distributed Amplifiaction," *Norwood, MA: Artech*, 1993

[45] E. W. Strid and K. R. Gleason, "A DC-12-GHz monolithic GaAs FET distributed amplifier," *IEEE Trans. Microwave Theory Tech.*, vol. 30, pp. 969-975, July 1982

[46] Y. Ayasli, R. L. Mozzi, J. L. Vorhaus, L. D. Reynolds, and R. A. Pucel, "A monolithic GaAs 1-13-GHz traveling-wave amplifier," *IEEE Trans. Microwave Theory Tech.*, vol. 30, pp.976-981, July 1982

[47] Y. C. Chen and S. S. Lu, "Analysis and Design of CMOS Broadband Amplifier with Dual Feedback Loops," *IEEE ASIC Proceedings Conference*, pp. 245 –248, 2002

[48] A. Worapishet, M. Chongcheawchamnan, and S. Srisathit,"Broadband amplification in CMOS technology using cascaded single-stage distributed amplifier," *Electronics Letts*, Vol. 38, pp. 675 –676 Jul. 2002

[49] F. Bruccoleri, E. A. M. Klumperink, and B. Nauta, "Noise Cancelling in Wideband CMOS LNAs," *IEEE Solid-State Circuits Conference*, Vol. 1, pp. 406 -407 2002

[50] J. Y. C. Chang, A. A. Abidi, and M. Gaitain, "Large Suspended Inductors on Silicon and Their use in a 2-um CMOS RF Amplifier," *IEEE Electronics Device Lett.,* vol. 14, pp. 246-248, May 1993

[51] C. K. Wang, P. C. Huang, and C. Y. Huang, "A fully differential CMOS transconductance-transimpedance wideband amplifier," *IEEE Transactions on Circuits and Systems II: Analog and Digital Signal Processing*, Vol. 42, pp. 745 -748, Nov 1995

[52] F. O. Eynde, and W. Sansen, "A CMOS wideband amplifier with 800 MHz gain-bandwidth," *IEEE Custom Integrated Circuits Conference Proceedings*, pp. 9.1/1 -9.1/4, 12-15, May 1991

[53] P. B. M. Hammer and P. M. Bakken, "2.4GHz CMOS VCO with multiple tuning inputs," *Electron. Lett.,* Vol. 38, pp. 874-876, 2002.

[54] T. K. Lin, and A. J. Payne, "Design of a Low-Voltage, Low-Power, Wide-Tuning Integrated Oscillator," *IEEE ISCAS,* pp. V-629-V-632, 2000.

[55] X. Haiqiao, and S. Rolf, "A Low-Voltage Low-Power CMOS 5-GHz Oscillator Based on Active Inductors," *Proc. IEEE*, pp. 231-234, 2002.

[56] C. Park and B. Kim, "A low-noise 900MHz VCO in 0.6um CMOS," in *VLSI Circuit Sym. Dig. Tech.* Papers pp. 28-29 1998.